

Midlatitude stratosphere - troposphere exchange as diagnosed by MLS O3 and MOPITT CO assimilated fields

L. El Amraoui, Jean-Luc Attié, N. Semane, M. Claeyman, V.-H. Peuch, J. Warner, P. Ricaud, Jean-Pierre Cammas, A. Piacentini, B. Josse, et al.

▶ **To cite this version:**

L. El Amraoui, Jean-Luc Attié, N. Semane, M. Claeyman, V.-H. Peuch, et al.. Midlatitude stratosphere - troposphere exchange as diagnosed by MLS O3 and MOPITT CO assimilated fields. Atmospheric Chemistry and Physics, 2010, 10, pp.2175-2194. 10.5194/acp-10-2175-2010 . meteo-00461842

HAL Id: meteo-00461842

https://meteofrance.hal.science/meteo-00461842

Submitted on 25 Oct 2016

HAL is a multi-disciplinary open access archive for the deposit and dissemination of scientific research documents, whether they are published or not. The documents may come from teaching and research institutions in France or abroad, or from public or private research centers.

L'archive ouverte pluridisciplinaire **HAL**, est destinée au dépôt et à la diffusion de documents scientifiques de niveau recherche, publiés ou non, émanant des établissements d'enseignement et de recherche français ou étrangers, des laboratoires publics ou privés.

Atmos. Chem. Phys., 10, 2175–2194, 2010
www.atmos-chem-phys.net/10/2175/2010/
© Author(s) 2010. This work is distributed under
the Creative Commons Attribution 3.0 License.

Atmospheric Chemistry and Physics

Midlatitude stratosphere – troposphere exchange as diagnosed by MLS O_3 and MOPITT CO assimilated fields

L. El Amraoui[1], J.-L. Attié[1,2], N. Semane[3], M. Claeyman[1,2], V.-H. Peuch[1], J. Warner[4], P. Ricaud[2], J.-P. Cammas[2], A. Piacentini[5], B. Josse[1], D. Cariolle[5], S. Massart[5], and H. Bencherif[6]

[1]CNRM-GAME, Météo-France and CNRS, URA 1357, Toulouse, France
[2]Laboratoire d'Aérologie, Université de Toulouse, CNRS/INSU, Toulouse, France
[3]CNRM, Direction de la Météorologie Nationale, Casablanca, Morocco
[4]University of Maryland, Baltimore County, USA
[5]CERFACS, Toulouse, France
[6]Laboratoire de l'Atmosphère et des Cyclones, Université de La Réunion, France

Received: 5 June 2009 – Published in Atmos. Chem. Phys. Discuss.: 1 October 2009
Revised: 12 February 2010 – Accepted: 16 February 2010 – Published: 2 March 2010

Abstract. This paper presents a comprehensive characterization of a very deep stratospheric intrusion which occurred over the British Isles on 15 August 2007. The signature of this event is diagnosed using ozonesonde measurements over Lerwick, UK (60.14° N, 1.19° W) and is also well characterized using meteorological analyses from the global operational weather prediction model of Météo-France, ARPEGE. Modelled as well as assimilated fields of both ozone (O_3) and carbon monoxide (CO) have been used in order to better document this event. O_3 and CO from Aura/MLS and Terra/MOPITT instruments, respectively, are assimilated into the three-dimensional chemical transport model MOCAGE of Météo-France using a variational 3-D-FGAT (First Guess at Appropriate Time) method. The validation of O_3 and CO assimilated fields is done using self-consistency diagnostics and by comparison with independent observations such as MOZAIC (O_3 and CO), AIRS (CO) and OMI (O_3). It particularly shows in the upper troposphere and lower stratosphere region that the assimilated fields are closer to MOZAIC than the free model run. The O_3 bias between MOZAIC and the analyses is −11.5 ppbv with a RMS of 22.4 ppbv and a correlation coefficient of 0.93, whereas between MOZAIC and the free model run, the corresponding values are 33 ppbv, 38.5 ppbv and 0.83, respectively. In the same way, for CO, the bias, RMS and correlation coefficient between MOZAIC and the analyses are −3.16 ppbv, 13 ppbv and 0.79, respectively, whereas between MOZAIC and the free model they are 6.3 ppbv, 16.6 ppbv and 0.71, respectively. The paper also presents a demonstration of the capability of O_3 and CO assimilated fields to better describe a stratosphere-troposphere exchange (STE) event in comparison with the free run modelled O_3 and CO fields. Although the assimilation of MLS data improves the distribution of O_3 above the tropopause compared to the free model run, it is not sufficient to reproduce the STE event well. Assimilated MOPITT CO allows a better qualitative description of the stratospheric intrusion event. The MOPITT CO analyses appear more promising than the MLS O_3 analyses in terms of their ability to capture a deep STE event. Therefore, the results of this study open the perspectives for using MOPITT CO in the STE studies.

1 Introduction

The troposphere and the stratosphere are characterized by different dynamical and chemical properties, involving strong gradients of potential vorticity (PV), relative humidity (RH) and chemical species such as ozone (O_3) and carbon monoxide (CO) at the tropopause. Dynamical, chemical and radiative coupling between the stratosphere and the troposphere are among the most important processes that must be understood for prediction of climate change (Holton et al., 1995). Stratosphere-troposphere exchange (STE) events play a key role in controlling the ozone and water vapour budgets of the upper troposphere and lower stratosphere (UTLS) region. STE events can have a significant role in the radiative forcing of climate change in relation to the increase of

Correspondence to: L. El Amraoui
(laaziz.elamraoui@meteo.fr)

the anthropogenic influences (e.g. Santer et al., 2003). In this context, Stohl et al. (2003) reported that modifications in STE events in a changing climate may significantly affect stratospheric ozone depletion and the oxidizing capacity of the troposphere.

STE events have been reviewed by e.g. WMO (1986); Davies and Schuepbach (1994); Holton et al. (1995); Stohl et al. (2003). The exchange of mass across the tropopause is bidirectional, with a return flow transporting tropospheric air into the lowermost stratosphere (Danielsen, 1968; Hoor et al., 2002). It occurs via a variety of processes on different scales which include both Troposphere to Stratosphere Transport (TST) (e.g. Zahn et al., 2000; Hoor et al., 2002) and Stratosphere to Troposphere Transport (STT) (e.g. Danielsen, 1968; Shapiro, 1980) events. The TST events occur mainly in the tropics, and also at higher latitudes. The isentropic transport into the lowermost stratosphere takes place across the extratropical tropopause (Dessler et al., 1995) and the transport of tropospheric air into the stratosphere is irreversible (Hintsa et al., 1998). Conversely, the STT events happen everywhere but dominate in the midlatitudes. The deep descent of stratospheric air into the troposphere leads to irreversible transport as the stratospheric air becomes mixed with the surrounding air (Papayannis et al., 2005).

Stratospheric intrusions are the most important manifestations of STT events in the extratropics and they are associated with tropopause folds (Danielsen, 1968; Kentarchos et al., 1999). These events, characterized by tongues of anomalously high potential vorticity, are considered as the main sources of ozone into the troposphere. Stratospheric intrusions form in the baroclinic zone beneath a jet stream, as a result of an ageostrophic circulation forced by convergence at the jet entrance (Keyser and Shapiro, 1986). They mainly depend on small-scale near-tropopause processes and they are more frequent in the extratropical regions than further poleward (e.g. Sprenger et al., 2003; Rao and Kirkwood, 2005). The intruding stratospheric air typically forms filamentary structures, which appear as laminae in ozone profiles and can reveal mesoscale features on water vapour satellite images especially if they are stretched into streamers and subsequently roll up (Holton et al., 1995; Stohl et al., 2003).

Knowledge of the frequency and global geographical distributions of stratospheric intrusions is important for the climatological understanding of extratropical synoptic-scale and mesoscale weather systems, and of irreversible mixing between stratospheric and tropospheric air (Sprenger et al., 2003). For these reasons, they have been widely studied using in-situ aircraft measurements (e.g. Hoor et al., 2002; Brioude et al., 2006), ground-based lidar sounding data (e.g. Eisele et al., 1999), airborne lidar systems (e.g. Browell et al., 1987), in-situ ozonesonde stations (e.g. Seidel and Randel, 2006), meteorological analyses (e.g. Wernli and Bourqui, 2002; Sprenger et al., 2003), and modelling studies (e.g. Kentarchos et al., 1999; Hsu et al., 2005). Most of the studies dealing with tropopause folds focused on the detection of the stratospheric signature in the troposphere based on low RH and high O_3, PV, radioactivity (^{7}Be, ^{10}Be/^{7}Be) or static stability. Relationships between tracers have also been used in order to characterize mixing processes in the tropopause region (e.g. Zahn et al., 2000; Pan et al., 2007; Brioude et al., 2008).

Satellite measurements based on the analysis of satellite imagery from water vapour channels (e.g. Appenzeller, 1996; Wimmers et al., 2003) or the analysis of ozone total columns (e.g. Shapiro et al., 1987; Wimmers and Moody, 2004) have also been used in order to diagnose and document stratospheric intrusions into the troposphere. Generally, satellite measurements have the advantage that they provide global coverage which offers the opportunity to investigate the mixing processes between the stratosphere and the troposphere in the UTLS region. However, these measurements are not able to resolve the synoptic-scale variabilities in the tropopause region, neither from limb-viewing sensors because of their sparse horizontal sampling, nor from nadir-viewing sensors because of their poor vertical resolutions. Moreover, the UTLS region is characterized by very high vertical gradients. The representation of these gradients is a well-known limitation of most of the global chemical transport models (CTM) as described by Law et al. (2000) in their comparison between global CTM results and Measurement of OZone and wAter vapour by aIrbus in-service airCraft (MOZAIC) in-situ data (Marenco et al., 1998). Therefore, the use of chemical data assimilation, which allows for an optimal combination of model results and measurements, can be very useful to better resolve the UTLS region. In this context, Clark et al. (2007) and Semane et al. (2007) have used O_3 assimilated fields from MOZAIC in-situ measurements and stratospheric profiles from the Michelson Interferometer for Passive Atmospheric Sounding (MIPAS) instrument onboard ENVISAT, respectively, in order to better describe the exchange between the troposphere and the stratosphere across the tropopause region.

The main objectives of this paper are: firstly, to document a deep stratospheric intrusion event, which occurred over the British Isles on 15 August 2007, using ozonesonde measurements, meteorological analyses, as well as modelled and assimilated fields of O_3 and CO observations from the Microwave Limb Sounder (MLS) instrument onboard Aura satellite and from the Measurements Of the Pollution In The Troposphere (MOPITT) instrument onboard Terra satellite, respectively. Secondly, to evaluate the added-value of stratospheric O_3 and tropospheric CO assimilated fields in regard to the composition of the UTLS region and to STE events in comparison to modelled O_3 and CO fields from MOCAGE.

Thus, an original objective of this study is to evaluate the capacity to improve the description of STE events with the assimilation of the tropospheric CO field from MOPITT. To our knowledge, satellite CO data assimilation, in particular from the MOPITT instrument, has not yet been used in

scientific studies related to stratospheric intrusion events. We will then demonstrate the capability of CO assimilated fields from MOPITT to describe a deep stratospheric intrusion in comparison to MLS O_3 assimilated fields. Both O_3 and CO observations are assimilated into the 3-D-CTM MOCAGE of Météo-France using a variational 3-D-FGAT (First Guess at Appropriate Time) method within the MOCAGE-PALM assimilation system. This paper is outlined as follows. Section 2 presents the satellite observations as well as the model and the assimilation system used in this study. In Sect. 3, we characterize the aforementioned event with the help of ozonesonde measurements and meteorological data. Section 4 presents a validation of the O_3 and CO assimilated products in comparison with other independent data. The characterization of the stratospheric intrusion event with O_3 and CO assimilated fields is described in Sect. 5. Main results are summarized in Sect. 6.

2 Data and analysis

2.1 Aura/MLS ozone observations

The Aura satellite was launched on 15 July 2004 and placed into a near-polar Earth orbit at ∼705 km with an inclination of 98° and an ascending node at 13:45 h. It makes about 14 orbits per day. The MLS instrument onboard Aura uses the microwave limb sounding technique to measure chemical constituents and dynamical tracers between the upper troposphere and the lower mesosphere (Waters et al., 2006). It provides dense spatial coverage with 3500 profiles daily between 82° N and 82° S.

In this study we use the Version 2.2 of MLS O_3 dataset. It is a standard retrieval between 215 and 0.46 hPa with a vertical resolution of ∼3 km in the upper troposphere and the stratosphere. The along-track resolution of O_3 is ∼200 km between 215 and 10 hPa. The estimated single-profile precision in the extratropical UTLS region is of the order of 0.04 ppmv from 215 to 100 hPa and between 0.05 and 0.2 ppmv from 46 to 10 hPa. For the assimilation experiment, MLS data are selected according to the precision and quality flags recommended in the MLS Version 2.2 Level data quality and description document (see http://mls.jpl.nasa.gov/data/v2-2_data_quality_document.pdf). The respective errors for each profile are taken into account in the assimilation process through the error covariance matrix of observations. Note that only measurements performed between 215 and 10 hPa are used during the assimilation experiment because of the limitation imposed by the upper boundary of the used version of the MOCAGE model, namely 5 hPa.

2.2 Terra/MOPITT carbon monoxide observations

The MOPITT instrument (Drummond and Mand, 1996) is onboard the Terra platform and has been monitoring global tropospheric CO from March 2000 to date. These data have been intensively validated (e.g. Emmons et al., 2004, 2009). The pixel size is 22 km×22 km and the vertical profiles are retrieved on 7 pressure levels (surface, 850, 700, 500, 350, 250 and 150 hPa). The maximum likelihood method, used to retrieve the MOPITT CO, is a statistical combination of the measurements and a priori information (for more information about the MOPITT CO retrieval algorithm, see Deeter et al., 2003). The retrieval profiles are characterized by their averaging kernels, which provide information on the vertical sensitivity of the measurements. In this study, we consider MOPITT CO (Version 3) retrievals with less than 40% a priori contamination to insure a consistent and good quality dataset. MOPITT data are averaged in boxes of 2°×2° to obtain super-observations directly assimilated into the used version of MOCAGE-PALM system. Moreover, in order to take into account of the vertical resolution of the MOPITT measurements, their averaging kernels as well as their a priori profiles are considered in the assimilation procedure. Note that the variance-covariance error matrices of MOPITT measurements are also taken into account during the assimilation process through the error covariance matrix of the observations.

2.3 MOCAGE CTM and data assimilation system

The assimilation system used in this study is MOCAGE-PALM (e.g. El Amraoui et al., 2008a) developed jointly between Météo-France and CERFACS (Centre Européen de Recherche et de Formation Avancée en Calcul Scientifique) in the framework of the ASSET European project (Lahoz et al., 2007a). MOCAGE (MOdèle de Chimie Atmosphérique à Grande Echelle) (Peuch et al., 1999) is a 3-D-CTM which covers the planetary boundary layer, the free troposphere, and the stratosphere. It provides a number of optional configurations with varying domain geometries and resolutions, as well as chemical and physical parameterization packages. It has the flexibility to use several chemical schemes for stratospheric and tropospheric studies. MOCAGE is used for several applications: operational chemical weather forecasting in Météo-France (Dufour et al., 2004), tropospheric as well as stratospheric research studies (e.g. Josse et al., 2004; Michou et al., 2005; Ricaud et al., 2009a,b), and data assimilation research (e.g. Cathala et al., 2003; Pradier et al., 2006; Clark et al., 2007; Semane et al., 2007; El Amraoui et al., 2008a,b; Semane et al., 2009). In this study, MOCAGE is forced dynamically by external wind and temperature fields from the ARPEGE model analyses, the global operational weather prediction model of Météo-France (Courtier et al., 1991). The MOCAGE horizontal resolution used for this study is 2° both in latitude and longitude and the model uses a semi-Lagrangian transport scheme. It includes 47 hybrid (σ, P) levels from the surface up to 5 hPa, where $\sigma = P/P_s$; P and P_s are the pressure and the surface pressure, respectively. MOCAGE has a vertical resolution of about 800 m in the vicinity of the tropopause and in the lower

stratosphere. A detailed validation of the model using a large number of measurements during the Intercontinental Transport of Ozone and Precursors (ICARTT/ITOP) campaign was done by Bousserez et al. (2007).

The assimilation module used in this study is PALM (Projet d'Assimilation par Logiciel Multiméthode): a modular and flexible software, which consists of elementary components that exchange data (Lagarde et al., 2001). It manages the dynamic launching of the coupled components (forecast model, algebra operators and input/output of observational data) and the parallel data exchanges. The technique implemented within PALM and used for the assimilation of O_3 and CO profiles from MLS and MOPITT, respectively, is the 3-D-FGAT method. This method is a compromise between the well-known 3-D-Var and 4-D-Var techniques (Fisher and Andersson, 2001). It compares the observation and background at the correct time and assumes that the increment to be added to the background state is constant over the entire assimilation window. The choice of this assimilation technique limits the size of the assimilation window, since it has to be short enough compared to chemistry and transport timescales. Using ozone profiles from the MIPAS instrument, this technique has already produced good-quality results compared to independent data and many other assimilation systems (e.g. Geer et al., 2006).

The assimilation system MOCAGE-PALM has been used to assess the quality of satellite ozone measurements (Massart et al., 2007). It has also been proven to be useful to overcome the possible deficiencies of the model. In this context, its assimilation product has been used in many atmospheric studies in relation to the ozone loss in the Arctic vortex (El Amraoui et al., 2008a), the tropics-midlatitudes exchanges (Bencherif et al., 2007), the stratosphere-troposphere exchanges (Semane et al., 2007), and the exchange between the polar vortex and the midlatitudes (El Amraoui et al., 2008b).

3 In-situ measurements and meteorological conditions during the stratospheric intrusion event

3.1 Ozonesonde measurements of the ozone anomaly over Lerwick on 15 August 2007

In this section, with the help of ozonesonde measurements, we characterize a positive anomaly of ozone in the UTLS region which occurred over the British Isles on 15 August 2007. At 12:00 UTC, an ozonesonde was launched from Lerwick (60.14° N, 1.19° W) as a part of the VINTERSOL (Validation of INTERnational Satellites and study of Ozone Loss) European field campaign. Figure 1a shows the volume mixing ratio profile of ozone over Lerwick (thick line) recorded on 15 August 2007. It also depicts a mean profile (thin line), which corresponds to the average of all August ozone profiles measured between 2004 and 2007.

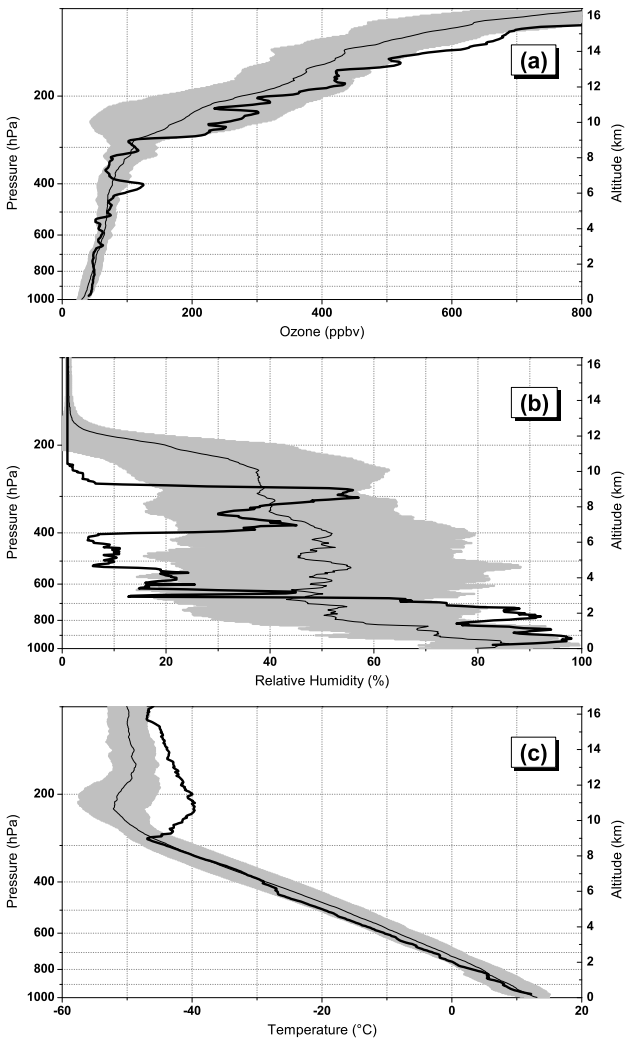


Fig. 1. **(a)** Thick line: Ozone volume mixing ratio profile in parts per billion by volume (ppbv) as obtained over Lerwick, UK (60.14° N, 1.19° W) in the British Isles on 15 August 2007 at 12:00 UTC from ozonesonde; **(b)** same as (a) but for relative humidity in %; **(c)** same as (a) but for temperature in Celsius degrees (°C). In (a–c), thin lines correspond to the average of all August profiles from 2004 to 2007. The shaded surface represents $\pm\sigma$ with respect to the mean profile.

The shaded area represents the standard deviation ($\pm\sigma$) with respect to the mean of all August profiles (2004–2007). The measured ozone profile on 15 August 2007 over Lerwick shows a positive ozone anomaly of the same order as the standard deviation in comparison to the mean profile especially between ∼280 and 120 hPa. Moreover, simultaneous ozonesonde measurements show very low relative humidity values (RH<5%) from the stratosphere down to about 280 hPa compared to the mean August profile as illustrated in Fig. 1b. Similarly, Figure 1c shows the temperature profile over the same location on 15 August 2007. The tropopause height on 15 August 2007, as indicated by

reversal in temperature gradient, is low compared to the average of all August profiles. Its downward displacement is estimated to be about 2 km. Finally, Fig. 1 shows just below 400 hPa a layer, which is ozone-rich, 1 km thick, very dry, and associated with a break in the vertical temperature lapse rate at approximately 6 km, which corresponds to the isentropic level of about 315 K. All the characteristics of this layer suggest the existence of a tropopause fold below the anomalously low-altitude tropopause. This is a clear signature of a strong baroclinic development event which is very likely associated with a STE event. In the next sections, we will document this event using meteorological analyses from the ARPEGE model as well as assimilated fields of O_3 and CO from the MLS and MOPITT instruments, respectively.

3.2 Meteorological conditions during the stratospheric intrusion event

The purpose of this section is to document the stratospheric intrusion which took place on 15 August 2007 over the northern British Isles with the help of the meteorological parameters. We give a dynamical context concerning the O_3 anomaly observed in the ozonesonde measurements and presented in Sect. 3.1. According to Hoskins et al. (1985), an upper-level cyclonic PV anomaly is associated with a decrease of the tropopause height. Therefore, the signature of stratospheric air descending to lower altitude levels can be seen in the potential vorticity field plotted on isentropic surfaces. Figure 2 top shows a PV isentropic map at 315 K on 15 August 2007 at 12:00 UTC from the ARPEGE analyses. It shows high values of PV over northern Great Britain which corresponds to an anomaly of the cyclonic PV at the tropopause (=1.5 pvu) where the PV maximum is located near the northern British Isles. Also note on Fig. 2 top the strip of 1.5 potential vorticity units (pvu) stretching from western Spain to southern England which will be further below associated with the upper level dynamics of a tropopause fold. Figure 2 bottom shows a zonal vertical cross-section (longitude versus pressure) across the region of lowest altitude tropopause described by the Lerwick ozonesonde measurements. As expected, the tropopause decreases with height particularly between the longitude range 0–10° W due to the strong cyclonic PV anomaly occurring above. In this region of the lowest altitude tropopause along the upper level trough (as low as about 430 hPa), rapid mixing by turbulence and convection may lead to irreversible STE events (Gouget et al., 2000).

ARPEGE analyses are used in order to describe the synoptic conditions during the stratospheric intrusion event. Figure 3 shows analyses of geopotential height (Fig. 3a), and potential temperature (Fig. 3b) on the potential vorticity iso-surface 1.5 pvu. In addition, the horizontal wind (both velocity and direction) and the relative humidity at 250 hPa pressure level are presented in Fig. 3c and d, respectively. The meteorological conditions show a typical

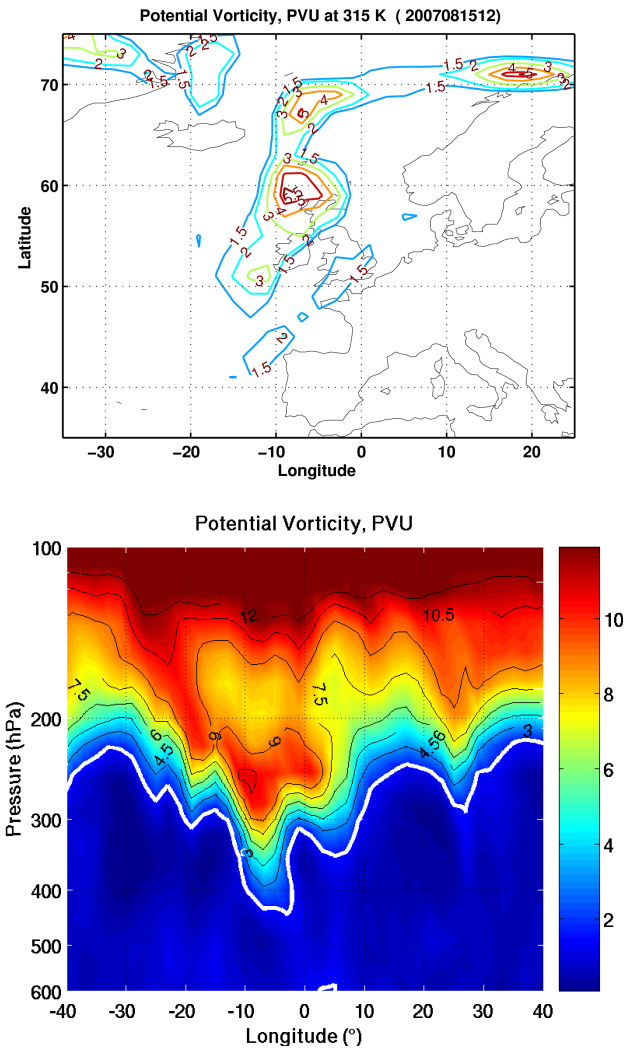


Fig. 2. (Top) Longitude-latitude cross-section of the Potential Vorticity (PV) field in PV units (pvu) on the 315 K isentropic level. Contours of PV are shown for values greater than 1.5 pvu. (Bottom) zonal cross-section of PV in longitude versus pressure at 61° N between 40° W and 40° E in longitude, and between 600 and 100 hPa in the vertical. Contours of PV are shown in black lines with an interval of 1.5 pvu. The white bold solid line corresponds to 1.5 pvu contour and indicates the height of the tropopause according to Hoskins et al. (1985). Note that the PV field for both figures is from the ARPEGE analyses corresponding to 15 August 2007 at 12:00 UTC.

baroclinic wave developing over western Europe with an intense trough extending from northeast of Iceland to northwest of Spain (Fig. 3a) and with jet-streaks on both sides of the upper-level trough (Fig. 3d). This trough isolates many tongues characterized by low values of geopotential height and potential temperature (see Fig. 3a and b). Above Lerwick, the region of the ozonesonde measurements (see Fig. 1), the dynamical tropopause (1.5 pvu iso-surface) descends to as low as 6.5 km altitude (Fig. 3a). This is

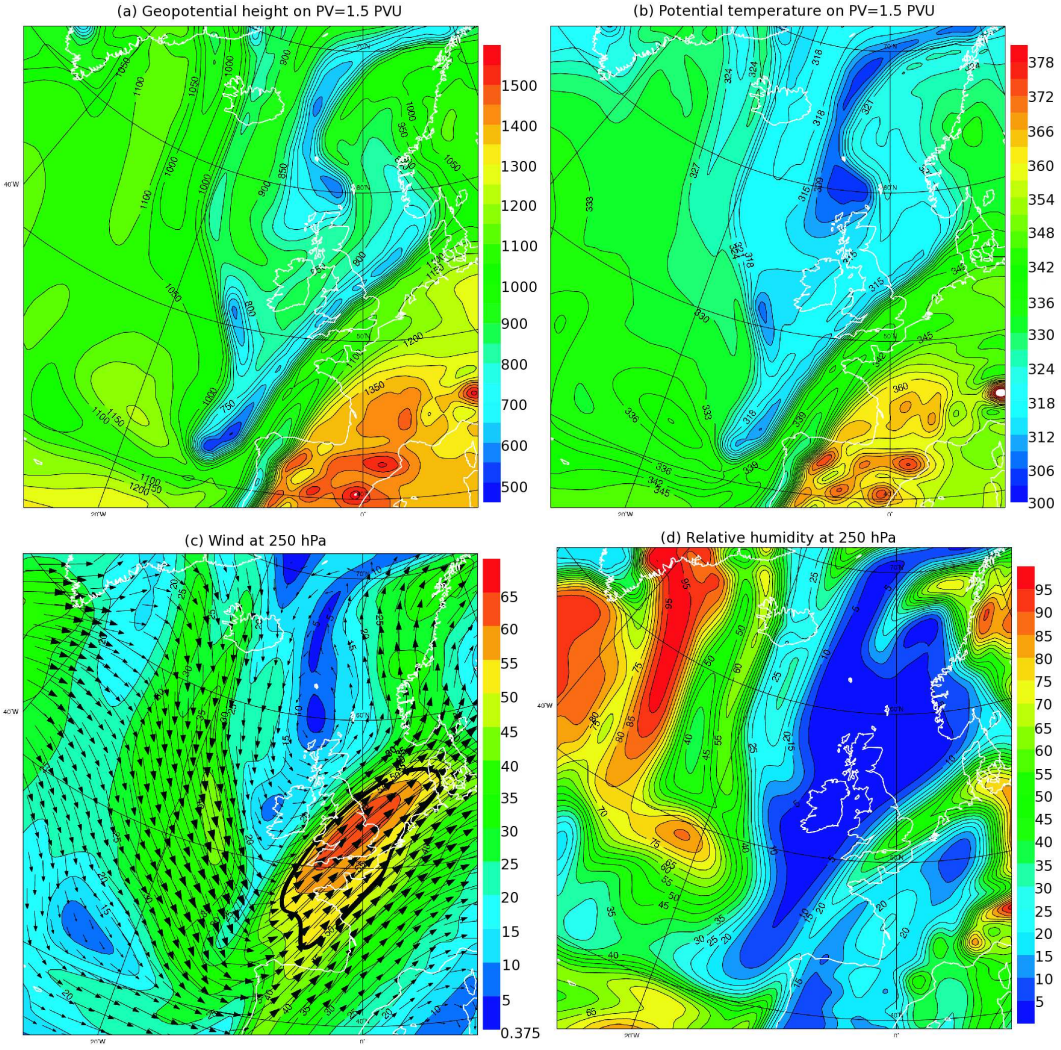


Fig. 3. Synoptic situation on 15 August 2007 at 12:00 UTC from the ARPEGE analyses. **(a)** Geopotential height in decameters (dam) (contour interval is 50 dam) on the potential vorticity (PV) iso-surface 1.5 PV units (pvu). **(b)** Potential temperature in Kelvin (K) on the same iso-surface as (a). Note that the 1.5 pvu iso-surface is an estimate of the dynamical tropopause according to Hoskins et al. (1985). **(c)** Horizontal wind direction (grey arrow) and velocity in m/s (coloured surface) at 250 hPa pressure level. Areas of velocities greater than 50 m/s are delimited by a bold solid line showing an upper-level jet streak. **(d)** Relative humidity in % at 250 hPa pressure level. Note that in (a–d), blue and red colours represent relatively low and relatively high values, respectively.

the level where physical processes may lead to irreversible STE event. In addition, there is also a tropopause break from 10 km altitude down to 6.5 km altitude (Fig. 3a) stretching a line along the cyclonic-shear side of the eastern jet streak (Fig. 3b) from northwest of Spain to East of Denmark. The tropopause break and the parallel PV band stretching on 315 K (Fig. 2) are dynamical signatures of on-going upper-level frontogenesis and tropopause folding (Keyser and Shapiro, 1986). This kind of fold is generally a consequence of an ageostrophic circulation near a jet streak, where the air from the lower stratosphere is intruded into the troposphere. In our case, we notice horizontal winds in excess of 50 m/s, showing an upper-level jet streak with southwest winds from the north of Spain to the west of Denmark at the 250 hPa pressure level. As a consequence of this circulation, the stratospheric air enters the troposphere beneath the core of the jet and on its cyclonic (poleward) side. Characteristic signatures of the intruded air are high PV, low RH, high O_3 and low CO concentrations. Irreversible stratospheric intrusions may occur along the 315 K isentropic surface, as suggested by the ozone layer captured below the low tropopause on the ozonesonde measurements at Lerwick (see Fig. 1). In the following sections, we seek signatures of the upper level dynamics on the distribution of O_3 and CO by using modelled outputs, both in the free model run and with the assimilation of satellite observations.

4 Evaluation of O_3 and CO assimilated fields

Throughout all this study, the model is forced by winds, temperatures, humidity and surface pressure from the ARPEGE analyses. The comprehensive chemical scheme RACMOBUS used for the assimilation of O_3 and CO measurements includes both the tropospheric RACM (Stockwell et al., 1997) and the stratospheric REPROBUS schemes (Lefèvre et al., 1994) since we are interested in the exchange between the troposphere and the stratosphere.

The assimilation experiments for O_3 and CO started on 20 July 2007 and were entirely separate. The initialization field for this date has been obtained by a free model run (MOCAGE with the detailed RACMOBUS chemistry scheme) started from the April climatological initial field. Thus, for each species (O_3 and CO), we have a free model run spin-up of more than 3 months in addition to 25 days of data assimilation concerning each species before the date of the stratospheric intrusion event. We estimate this spin-up period to be sufficient enough to have both O_3 and CO fields well balanced with respect to the atmospheric chemistry and dynamics.

In this section, we evaluate the quality of MLS O_3 and MOPITT CO assimilated fields into the MOCAGE-PALM assimilation system. This evaluation is required to test several assumptions introduced into data assimilation and to check the consistency of the analyses to the observations.

Several diagnostics, which consist of self-consistency tests, have been developed to check the quality of the assimilation runs (Talagrand, 2003). The chi-square (χ^2) test enables assessment of the estimation of the observation and background error covariance matrices (e.g. Khattatov et al., 2000) as well as other parameters such as the model error growth (e.g. El Amraoui et al., 2004).

If the observation and background errors are Gaussian, which is the case in this study (see OMF diagnostics in Figs. 4a and 8a as well as their corresponding comments), the cost function at its minimum ($J_{\min}$) should have a χ^2 distribution with p degrees of freedom, and must be equal on average to $p/2$ (Bennett, 1992; Talagrand, 2003; Lahoz et al., 2007b). The χ^2 formula is then given by:

$$\chi^2 = \frac{J_{\min}}{p/2}$$

The cost function J is given by:

$$J(x) = \frac{1}{2}\left[x(t_0) - x^b(t_0)\right]^T \mathbf{B}^{-1}\left[x(t_0) - x^b(t_0)\right] + \frac{1}{2}\sum_{i=1}^{p}[y(t_i) - H(x(t_i))]^T \mathbf{R}_i^{-1}[y(t_i) - H(x(t_i))]$$

The first term on the right-hand side is the misfit to the background state and the second term represents the misfit to the observations. $x^b(t_0)$ and $y(t_i)$ are the background state at the initial time and the observation at the time t_i, respectively. **B** and **R** are the background and the observation error covariance matrices, respectively. H is the observation operator, generally non-linear, which maps the model state x to the measurement space, where y is located.

A value of χ^2 close to 1 indicates a good estimation of both error-covariance matrices, whereas a value of χ^2 lower (greater) than 1 implies an overestimation (underestimation)

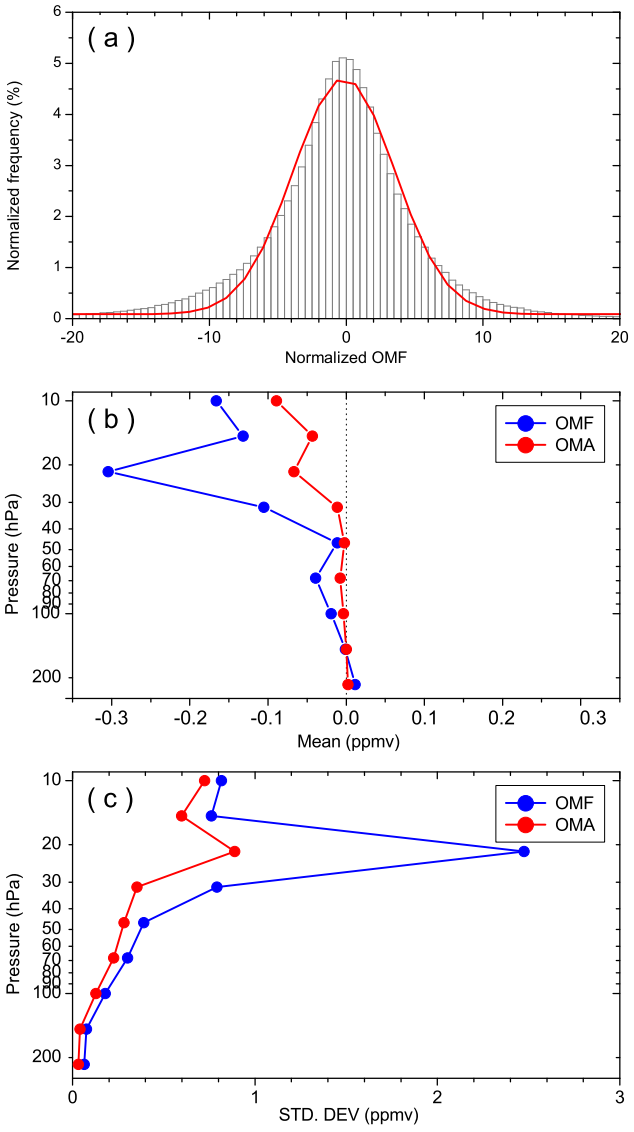


Fig. 4. (a) Histograms of observations minus forecasts (OMF) differences normalized by the observation error concerning assimilated MLS O_3. The red line is a Gaussian fit to the histogram. The good agreement between the histogram and the fit function supports the assumption of Gaussian errors in the observations and the forecast. **(b)** Vertical profile of the mean of OMF (blue) and OMA (red) both averaged over the assimilation period and over the globe for all MLS levels between 215 and 10 hPa. **(c)** The corresponding vertical profile of the standard deviations of OMF and OMA. Units in (b) and (c) are parts per million by volume (ppmv).

of the observation and/or background error covariance matrices. Another consistent self-diagnostic is based on observation minus analysis (OMA) residuals and observation minus forecast (OMF) innovations. This diagnostic, defined in the observation space, checks the consistency of both forecast and analysis distributions with respect to the observations (Lahoz et al., 2007b).

4.1 Validation of O_3 assimilated fields

The assimilation period in this study is between 20 July and 19 August 2007 during which the value of χ^2 for the O_3/MLS assimilation experiment varied between 0.81 and 1.22 with a mean value of 0.96. This result is satisfactory since it shows that both the observations and the background error covariance matrices were well estimated during the assimilation process.

Figure 4a shows the OMF distribution normalized by the observation errors for all MLS levels between 215 and 10 hPa corresponding to the assimilation period. The OMF histogram is fitted by a Gaussian function. The comparison between both the OMF histogram and the fitted Gaussian function is very good. This good agreement supports the assumption that the observations and the forecast have Gaussian errors. We note that the mean of normalized OMF values is close to zero (~ -1) with a standard deviation of 13.2, which suggests that the bias between the model and the observations is very small. Indeed, if the mean of the OMF statistics is significantly different from zero, this indicates a bias in the model or the observations. Figure 4b shows the vertical profile of the mean of the OMF and OMA distributions as a function of the vertical pressure both averaged over the assimilation period and over all the globe. Figure 4c displays their corresponding standard deviations. The mean of OMA is closer to zero than that of OMF with a corresponding standard deviation which is small than that of OMF at all pressure levels. This indicates that the analyses are closer to the observations than the forecast. Consequently the assimilation of MLS profiles corrects the background state at all observation levels.

To further test the behaviour of the data assimilation system, assimilated fields of MLS O_3 observations have been compared to MOZAIC measurements. The MOZAIC programme was launched in January 1993. The measurements started in August 1994, with the installation of ozone and water vapour sensors aboard 5 commercial aircraft. In 2001, the instrumentation was upgraded by installing carbon monoxide sensors on all aircraft and a total odd nitrogen instrument (NO_y) aboard one aircraft. Ozone is measured by UV absorption (Thermo Instruments, Model 49–103). The instruments are calibrated before and after each period of deployment ($\sim$every 12 months) and in-flight quality control is achieved, both for bias and calibration factor, with a built-in ozone generator. A comparison of the first 2 years of MOZAIC data with data of the ozonesonde network showed good agreement (Thouret et al., 1998). For the measurement of CO, the infra-red (IR) gas filter correlation technique is employed (Thermo Environmental Instruments, Model 48CTL). This IR instrument provides excellent stability, which is important for continuous operation without frequent maintenance. The sensitivity of the instrument was improved by several modifications (Nédélec et al., 2003), achieving a precision of ± 5 ppbv or $\pm 5\%$ for a 30 s response time. A complete description of the MOZAIC programme may be found at http://mozaic.aero.obs-mip.fr/web/ and in the IGAC Newsletters (Cammas and Volz-Thomas, 2007).

The comparison of MLS O_3 assimilated field as well as model outputs to MOZAIC observations is made in terms of time-series over the assimilation period (20 July–19 August). Collocated MOZAIC observations as well as assimilated and modelled O_3 output are averaged over a constant time bin whatever the number of aircraft and the position of MOZAIC measurements. Each average is then plotted as a function of the day time. Assimilated fields are plotted with respect to their standard deviations. Note that only observations above the altitude pressure of 280 hPa are considered since we are interested in the tropopause layer (the cruise flight altitude pressure of MOZAIC aircrafts is around 200 hPa). Figure 5 shows the time-series of O_3 assimilated field with its standard deviation (shaded colour) as well as the free model run compared to MOZAIC data for a one month period. The behaviour of all datasets is consistent throughout the period of comparison. Nevertheless, assimilated fields are closer than the free model output to MOZAIC measurements. The bias, RMS and correlation coefficient between aircraft and assimilated O_3 are -11.5 ppbv, 22.4 ppbv and 0.93, respectively, whereas between aircraft and modelled O_3 they are 33 ppbv, 38.5 ppbv and 0.83, respectively. These results suggest that MOZAIC in-situ measurements and O_3 assimilated field are in good agreement in the UTLS region.

As an additional validation, the deduced total column from O_3/MLS assimilated field is compared to the total column measured by the OMI (Ozone Monitoring Instrument) sensor onboard Aura satellite (Levelt et al., 2006). OMI is a nadir-scanning instrument that detects backscattered solar radiance at visible (350–500 nm) and UV wavelength channels (270–314 nm and 306–380 nm) to measure O_3 column with near global coverage over the Earth with a spatial resolution of 13 km $\times$ 24 km at nadir (except for polar night latitudes).

Figure 6 shows a comparison between O_3 total columns deduced from OMI, MOCAGE free run, and MLS assimilated field corresponding to 15 August 2007. MOCAGE underestimates the amount of O_3 total column, whereas total columns from OMI and MLS assimilated field are nearly the same particularly over the British Isles. The average bias between OMI and free model run is positive with a value of 17.64 DobsonUnit (DU) and a corresponding RMS of 12.82 DU, whereas the average bias between OMI and assimilated field is negative with a value of -13.21 DU and

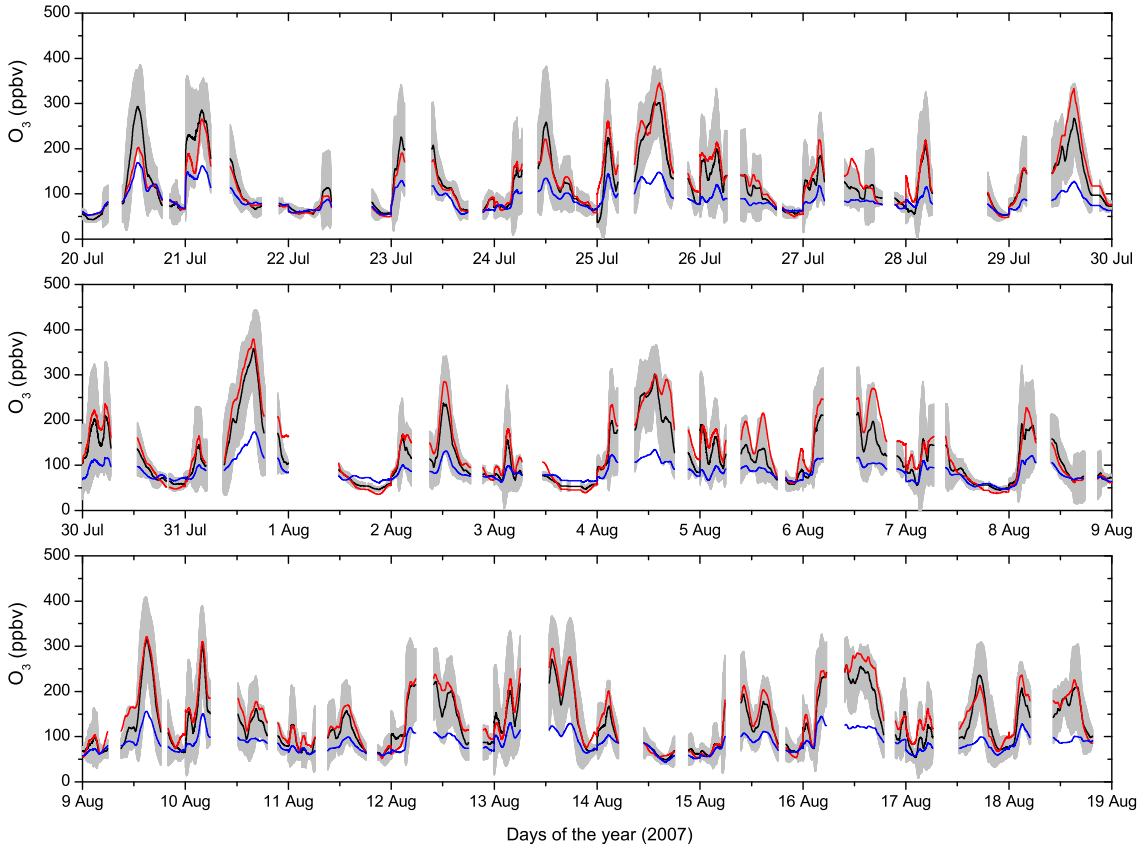


Fig. 5. Time-series of collocated MLS O_3 assimilated field (black) with its standard deviation (shaded colour) compared to MOZAIC measurements (red) and model free run output (blue) for the period: 20 July–19 August 2007. Only observations above the altitude pressure of 280 hPa are used for the comparison, since we are interested in the tropopause layer (the cruise flight altitude pressure of MOZAIC aircraft is around 200 hPa). Units: parts per billion by volume (ppbv).

a corresponding RMS of 12.10 DU. The correlation coefficient is 0.66 and 0.82 between OMI and free model run and between OMI and assimilated MLS, respectively.

The validation exercise with MOZAIC and OMI datasets confirms that the assimilation of O_3 from the MLS instrument improves the O_3 distribution, particularly in the UTLS region. This O_3 product will be used later in order to characterize the depth of the stratospheric intrusion in comparison to the PV field.

In order to assess the improvement of the ozone distribution in the UTLS region via the assimilation process, ozone profiles from both the free model run and the MLS assimilated field are compared with ozonesonde observations over Lerwick. The results of that comparison is given in Fig. 7. This figure clearly shows that the model underestimates the O_3 concentrations particularly between 300 and 150 hPa. The assimilation of MLS O_3 profiles corrects well this underestimation since the agreement between ozonesonde measurements and MLS assimilated profile is very good. The MLS analysis profile captures well the stratospheric intrusion event in the pressure levels between 180 and 270 hPa. However, between 400 and 430 hPa where ozonesonde observations (see also Fig. 1) depict a tropopause fold event, neither the model free run nor the O_3 MLS assimilation succeeds in capturing this STE event.

In the next section, we will check the capability of CO assimilated field to represent the characteristics of the stratospheric intrusion event.

4.2 Validation of CO assimilated fields

Concerning the assimilation of MOPITT CO, the value of χ^2 varied between 0.4 and 0.6. This shows that the observation and/or background error covariance matrices are somewhat overestimated in our assimilation experiment. To try to converge towards a value as close as possible to 1, we conducted several tests with different values of the background error which show that the variation of this parameter has little effect on the value of χ^2. Thus, the low value of χ^2 is most likely due to the overestimation of the error covariance matrices of MOPITT observations. Despite this fact, we prefer working with the actual error covariance matrices of the retrieved MOPITT CO since (i) they are a consistent characteristic of MOPITT that takes into account

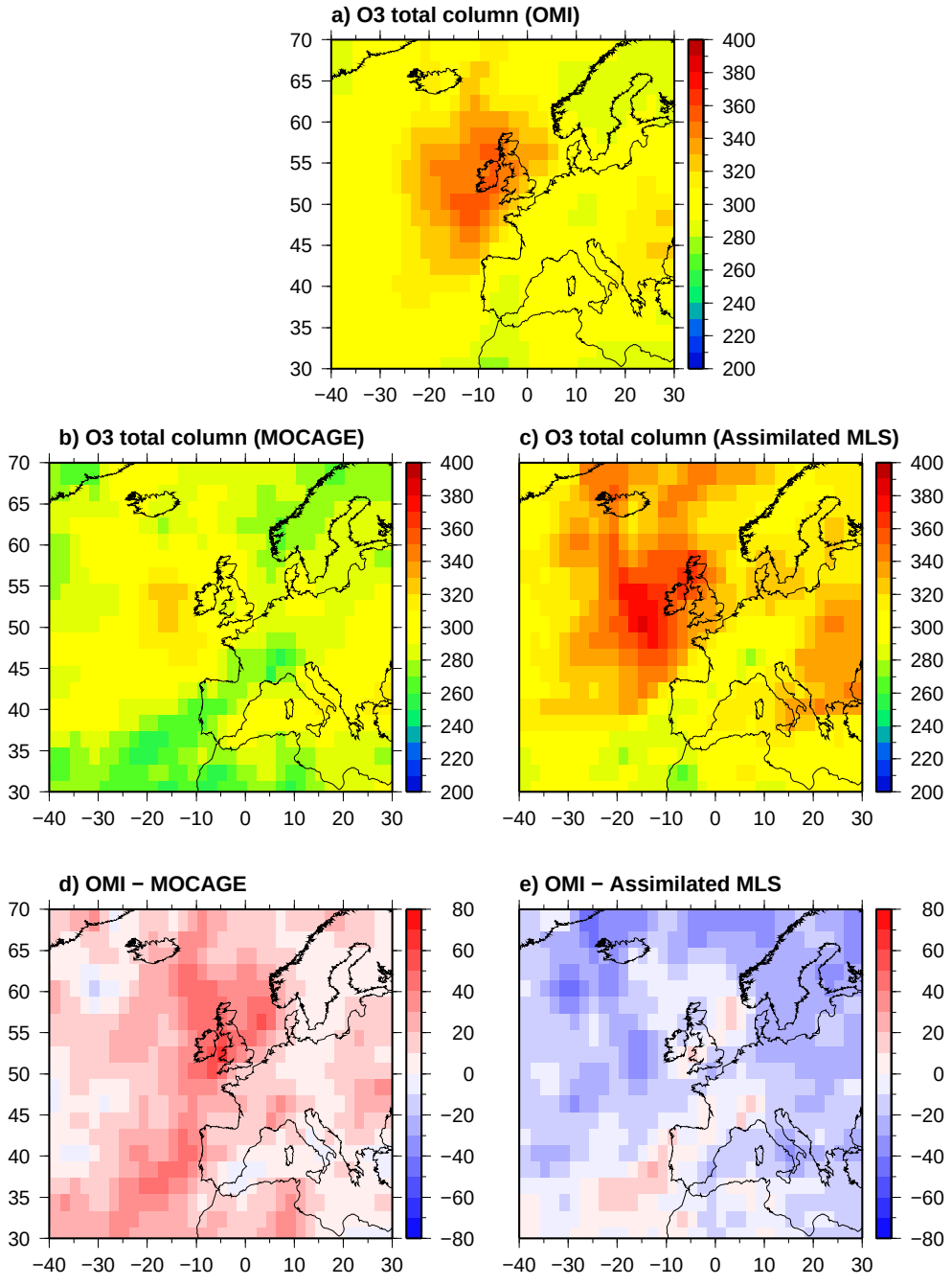


Fig. 6. Map of O_3 total column for 15 August 2007 as deduced from: **(a)** the OMI instrument, **(b)** MOCAGE free model run and **(c)** assimilated MLS O_3. **(d)** and **(e)** difference between OMI and MOCAGE and between OMI and assimilated MLS O_3 data, respectively. All datasets are binned into $2° \times 2°$. Blue and red colours in (d) and (e) indicate negative and positive differences, respectively. Units in all plots: DobsonUnit(DU).

many considerations: instrument characteristics, retrieval algorithm and validation, and (ii) the MOPITT assimilated field gives satisfactory results in comparison to independent data (see Figs. 9 and 10 and their associated comments). Figure 8 is similar to Fig. 4 but for MOPITT CO assimilated field. Figure 8a presents the OMF distribution normalized with the observation error for all MOPITT levels between the ground and 150 hPa corresponding to the assimilation period between 20 July and 19 August 2007. Similar conclusions as for MLS O_3 assimilated fields can be deduced. The fitted Gaussian function agrees well with the normalized OMF distribution. This supports the assumption of normally distributed observation and background errors. The mean of the normalized OMF values is close to zero (0.09) with a

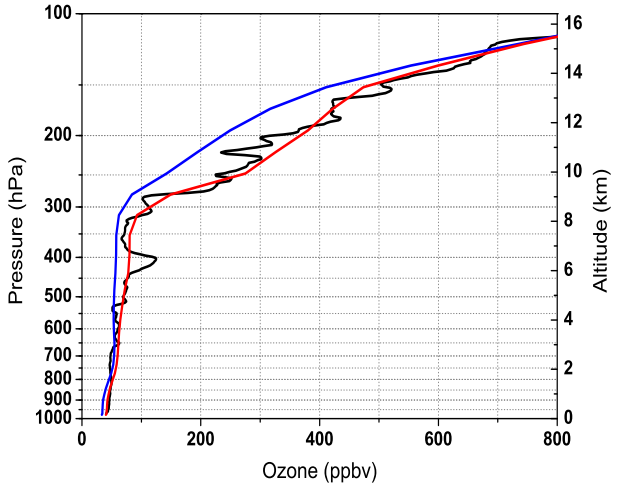


Fig. 7. Ozone volume mixing ratio profile in parts per billion by volume (ppbv) as obtained over Lerwick, UK (60.14° N, 1.19° W) in the British Isles on 15 August 2007 at 12:00 UTC from: ozonesonde measurements (black); free model run (blue) and assimilated MLS O_3 (red).

standard deviation of 9.8 suggesting that the bias between the model and the observations is very small. From Fig. 8b and Fig. 8c we can deduce that the mean of OMA vertical profile is closer to zero than that of OMF with a corresponding standard deviation which is small than that of OMF at all MOPITT pressure levels. This demonstrates again that the analyses are closer to the observations than the forecast.

All these results concerning the OMF and the OMA statistics for both O_3/MLS and CO/MOPITT illustrate the capability of data assimilation to reduce the bias between the observations and the model, and therefore adds value.

To validate the CO assimilated fields, we compare them to in-situ MOZAIC measurements in terms of time-series and vertical profiles. For time-series comparison, the same methodology is applied as for O_3 comparison (see Sect. 4.1). Figure 9 shows the time-series of MOPITT CO assimilated field with its standard deviation (shaded colour) as well as modelled CO free run compared to MOZAIC data over the same period as for O_3. Again, only observations above the altitude pressure of 280 hPa are considered. We note from Fig. 9 that the assimilation of MOPITT improves the CO model distribution in the UTLS. The behaviour of assimilated CO and MOZAIC is the same over the whole period of comparison and MOZAIC measurements remain generally inside the standard deviation of CO assimilated field. The maxima and the minima of CO are well localized in both datasets. The bias, RMS and correlation coefficient between aircraft and assimilated CO are −3.16 ppbv, 13 ppbv and 0.79, respectively, whereas between aircraft and modelled CO they are 6.3 ppbv, 16.6 ppbv and 0.71, respectively. This suggests that MOZAIC in-situ measurements and assimilated CO are in good agreement in the UTLS region.

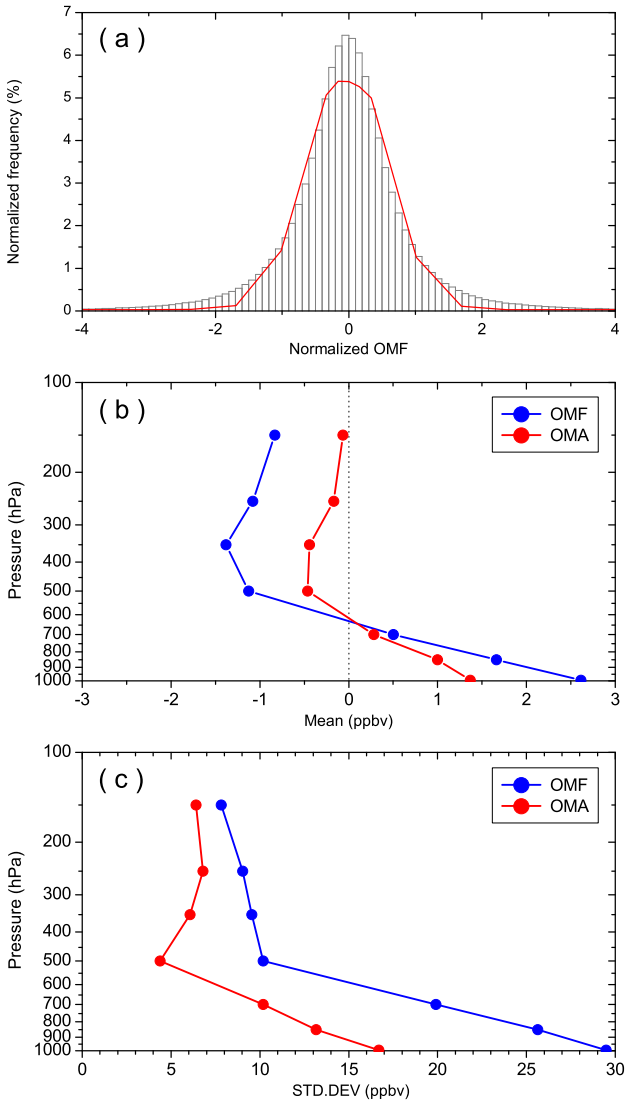


Fig. 8. (a) Histograms of observations minus forecasts (OMF) differences normalized by the observation error concerning assimilated MOPITT CO. The red line is a Gaussian fit to the histogram. The good agreement between the histogram and the fit function supports the assumption of Gaussian errors in the observations and the forecast. **(b)** Vertical profile of the mean of OMF (blue) and OMA (red) both averaged over the assimilation period and over the globe for all MOPITT levels between the ground and 150 hPa. **(c)** The corresponding vertical profile of the standard deviations of OMF and OMA. Units in (b) and (c) are parts per billion by volume (ppbv).

Another comparison was conducted with collocated vertical profiles for the three datasets over the only two MOZAIC airports visited over the whole assimilation period, Frankfurt, Germany (52.35° N, 14.55° E) and London, UK (51.3° N, 0.10° W). Note that collocated observations are selected in 2° radius area over both airports. The comparisons between MOZAIC, modelled free run and CO assimilated profiles over the two airports are shown in Fig. 10. Both comparisons

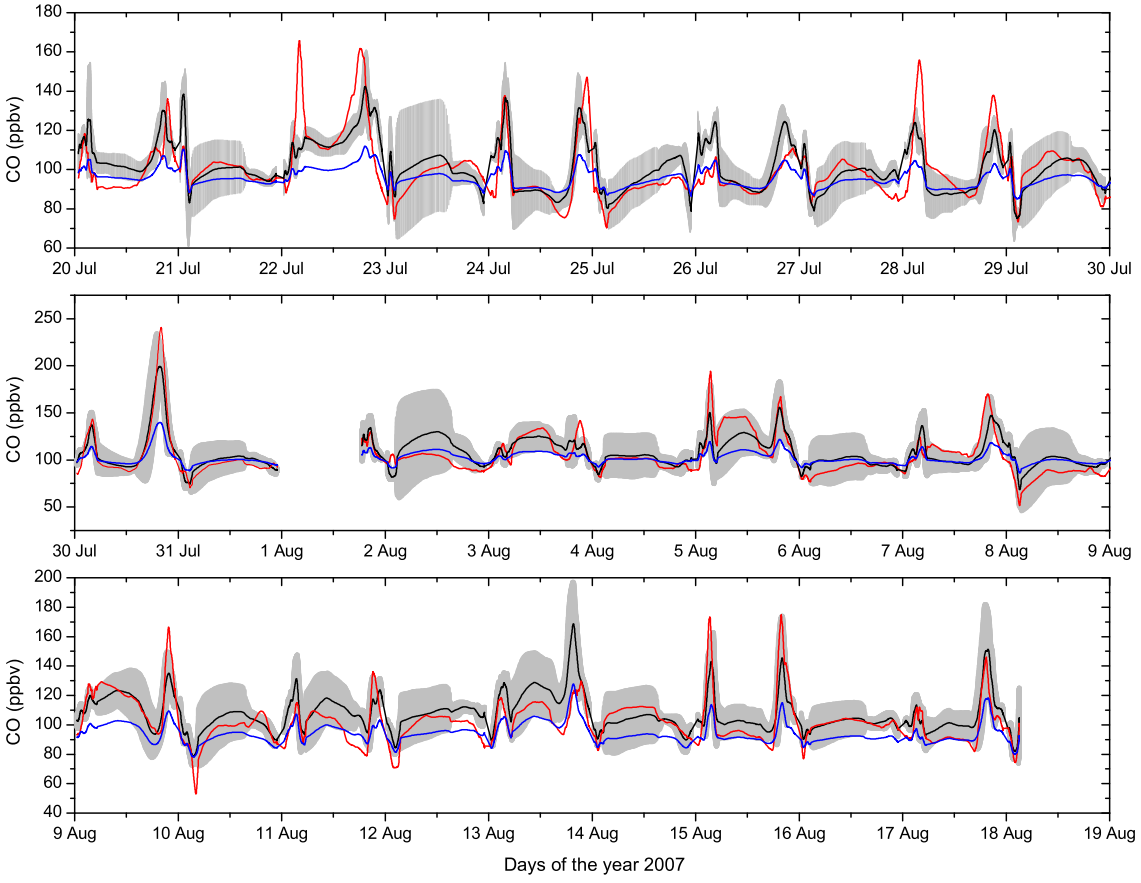


Fig. 9. Time-series of collocated MOPITT CO assimilated field (black) with its standard deviation (shaded colour) compared to MOZAIC measurements (red) and model free run output (blue) for the period: 20 July–19 August 2007. Only observations above the altitude pressure of 280 hPa are used for the comparison, since we are interested in the tropopause layer. Units: parts per billion by volume (ppbv).

show a very good agreement between MOZAIC and CO assimilated profiles. Over Frankfurt, the bias, RMS and correlation coefficient between MOZAIC and assimilated CO are 3.3 ppbv, 7.6 ppbv and 0.95, respectively whereas between MOZAIC and modelled CO they are 10.4 ppbv, 8.1 ppbv and 0.89, respectively. Over London, the bias, RMS and correlation coefficient between MOZAIC and assimilated CO are 4.5 ppbv, 8.5 ppbv and 0.63, respectively whereas between MOZAIC and modelled CO they are 12.4 ppbv, 11.7 ppbv and 0.55, respectively. The difference between MOZAIC and assimilated profiles, for both locations, are very small at all altitudes and the vertical variability is almost similar for both datasets in the UTLS region.

After validating the assimilated CO product using MOZAIC in-situ data, we compared the total column deduced from assimilated CO to that retrieved from the Aqua/AIRS (Atmospheric Infrared Sounder) instrument. AIRS instrument onboard Aqua was launched in 2002 with its primary goal of determining the vertical profiles of temperature and water vapour in the Earth's atmosphere (Aumann et al., 2003). CO retrievals are obtained from the 2160–2200 cm^{-1} portion of the spectrum on the edge of the 1–0 vibration-rotation band of CO, and the AIRS retrieval method was described by Susskind et al. (2003) and McMillan et al. (2005). AIRS CO measurements are provided at approximately 45 km×45 km horizontal resolution and 1600 km swath, and therefore, combined with its cloud clearing capability, AIRS can obtain near daily global coverage. AIRS tropospheric CO profiles as well as the mixing ratios at 500 hPa have been compared with those of MOPITT (Warner et al., 2007). An average CO bias of 10–15 ppbv between AIRS and MOPITT observations is identified and the biases are mainly due to the prior information used in the retrieval algorithms.

Figure 11 presents the comparison between the results of MOCAGE free model run, the assimilation of MOPITT CO in MOCAGE-PALM and AIRS CO total column independent data. All datasets correspond to the average of 15 and 16 August 2007 data binned in 2°×2° boxes. The differences between assimilated and free model run are relatively large particularly in the western and the northern British Isles. Note that assimilated MOPITT and model free run are compared to AIRS CO data in order to have an idea about the quality of the assimilated field with respect to the free model

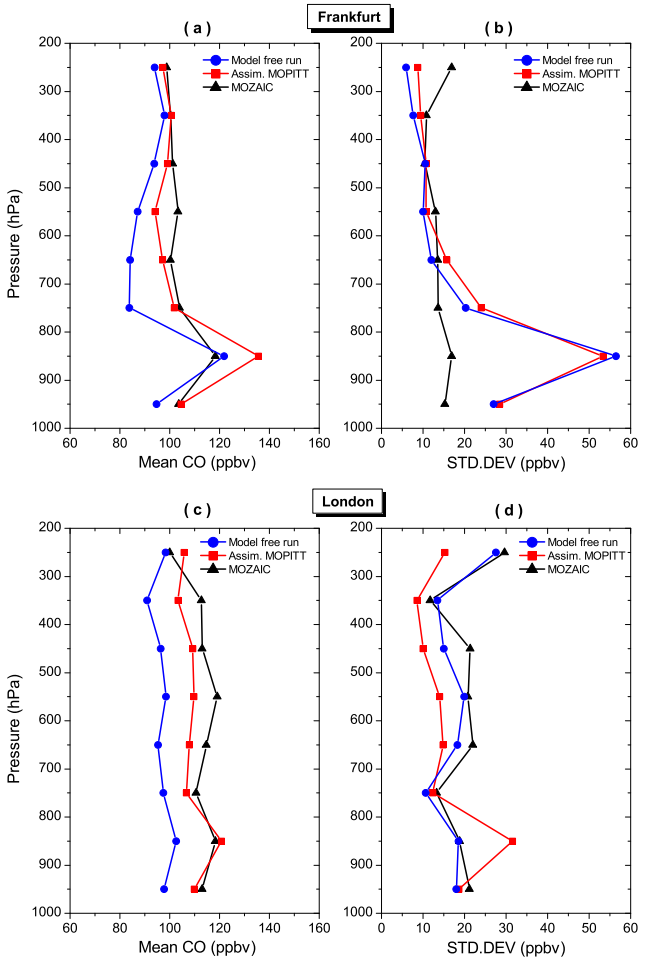


Fig. 10. **(a)** The mean CO vertical profiles in parts per billion by volume (ppbv) of MOPITT assimilated field (red), MOZAIC (black) and model free run (blue) over Frankfurt. All profiles are averaged over the assimilation period (20 July–19 August 2007) and within a geographical box of 2°×2° centred over the specified location. **(b)** the corresponding standard deviations. **(c)** and **(d)** are the same as (a) and (b), respectively, but for London.

run. The correlation coefficients between AIRS and modelled CO and between AIRS and assimilated MOPITT CO (without applying the AIRS averaging kernels) are 0.51 and 0.75, respectively. This shows that assimilated MOPITT CO is better than the free model run compared to the AIRS independent data. This figure shows the positive impact of MOPITT CO assimilation with an obvious improvement in terms of CO distribution. Total columns from AIRS and assimilated field almost show the same behaviour: a maximum of CO on the west side of the British Isles, and a minimum of CO over the British Isles and northward. These features are not present in the MOCAGE free model run. The good agreement between the assimilated CO MOPITT field and the AIRS data provides confidence in the MOCAGE-PALM results.

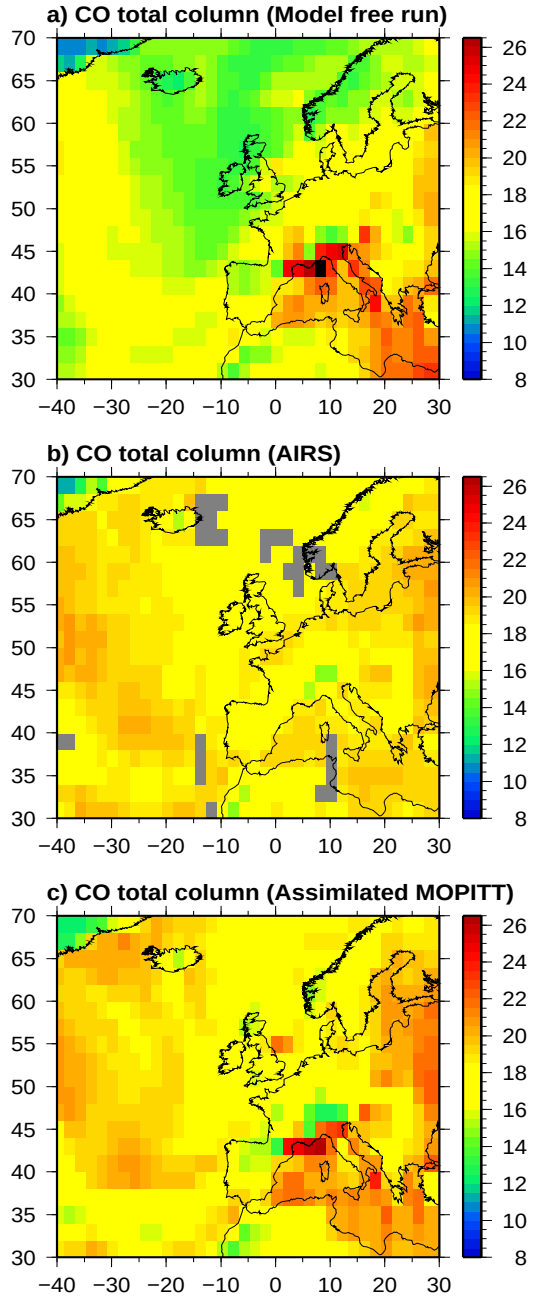


Fig. 11. Average CO total column field over 15 and 16 August 2007 as deduced from **(a)** the model free run, **(b)** AIRS instrument, and **(c)** assimilated MOPITT CO data. All datasets are binned into 2°×2°. The grey areas in (b) correspond to a lack of data in AIRS measurements. Note that no averaging kernel from AIRS is applied for neither MOCAGE nor assimilated product in this comparison. The correlation coefficient between AIRS and MOCAGE and between AIRS and assimilated MOPITT CO data are 0.51 and 0.75, respectively. Units in all plots: 10^{21} molec/m^2.

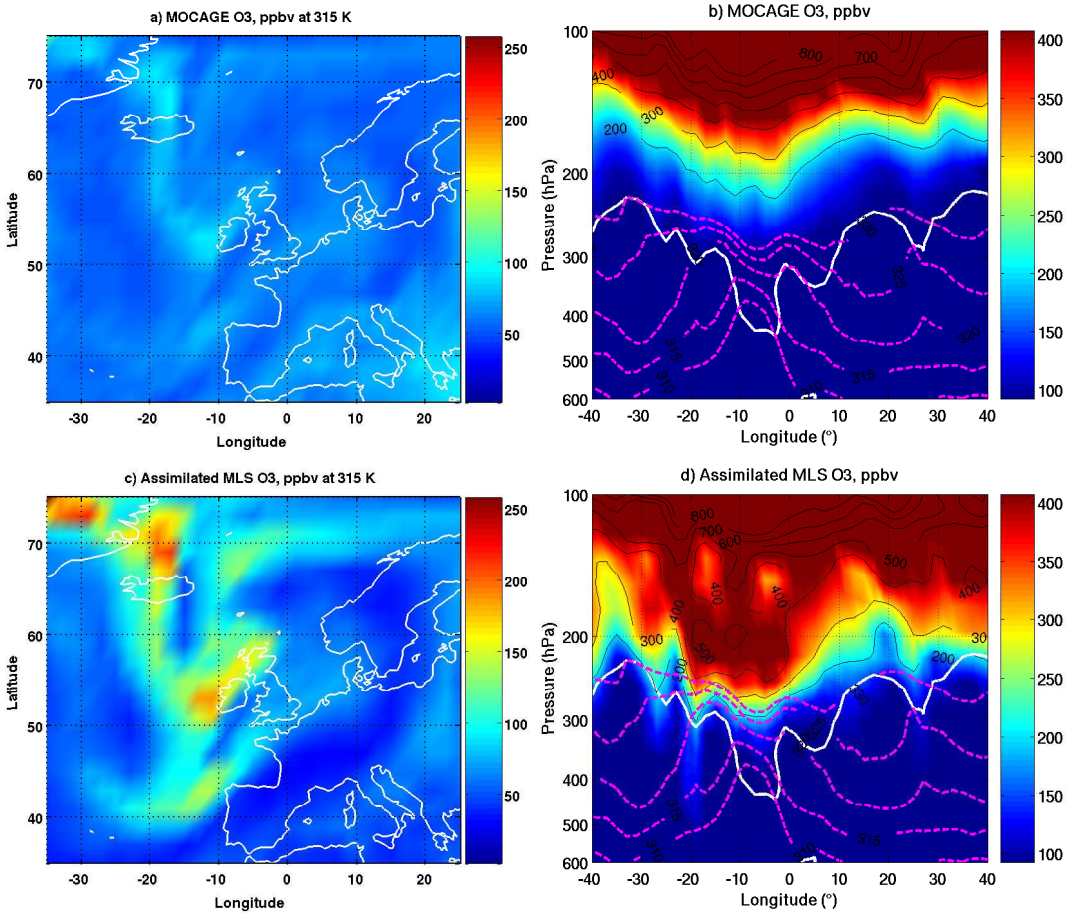


Fig. 12. **(a)** Longitude-latitude cross-section at the 315 K isentropic level of O_3 from MOCAGE. **(b)** Zonal cross-section of O_3 from MOCAGE in longitude versus pressure at 61° N between 40° W and 40° E in longitude, and between 600 and 100 hPa in the vertical. Contours of O_3 field are shown in thin black lines. The thick white line corresponds to 1.5 potential vorticity units contour: an estimate of the dynamical tropopause height. The magenta dashed lines correspond to the potential temperature contours between 310 and 330 K with an interval of 5 K from bottom to top. Both figures are for 15 August 2007 at 12:00 UTC. **(c)** and **(d)** are the same as (a) and (b), respectively, but for the MLS O_3 assimilated field. Units of O_3: parts per billion by volume (ppbv).

These validation tasks confirm that the MOPITT CO assimilated fields within MOCAGE-PALM is well suited for the study in relation with the stratospheric intrusion event.

5 Characterization of the stratospheric intrusion event with O_3 and CO assimilated fields

In this section, we focus on the comparison of the STE event representation as diagnosed in Sect. 3, with MOCAGE runs with and without assimilation of satellite data.

5.1 Signature of the stratospheric intrusion in O_3 assimilated fields

To look for the ozone signature indicating stratospheric intrusions, we analyse modelled and assimilated O_3 fields on isentropic maps and in vertical cross-sections (Fig. 12). The isentropic distribution of modelled O_3 over the domain of interest (Fig. 12a) is quite homogeneous. However, the upper level dynamics is associated with very weak maxima over the two regions of interest. Firstly, over northern UK where the positive anomaly of ozone in the lowermost stratosphere and the tropopause fold were observed (see Fig. 1), and secondly over northwestern Spain where a PV strip on the 315 K surface suggested the existence of a tropopause fold. The vertical cross-section north of UK (Fig. 12b) confirms a strong underestimation of modelled O_3 well above the dynamical tropopause (1.5 pvu isoline). This is due to the fact that there is no evidence of an ozone maximum in the 300–200 hPa layer between 10° W and 0° W, where the ozonesonde measurements (Fig. 1) indicated a positive ozone anomaly. Further, at 400 hPa, where a tropopause fold is suggested on the ozone sounding (Fig. 1), there is less signature of a stratospheric intrusion in the modelled O_3

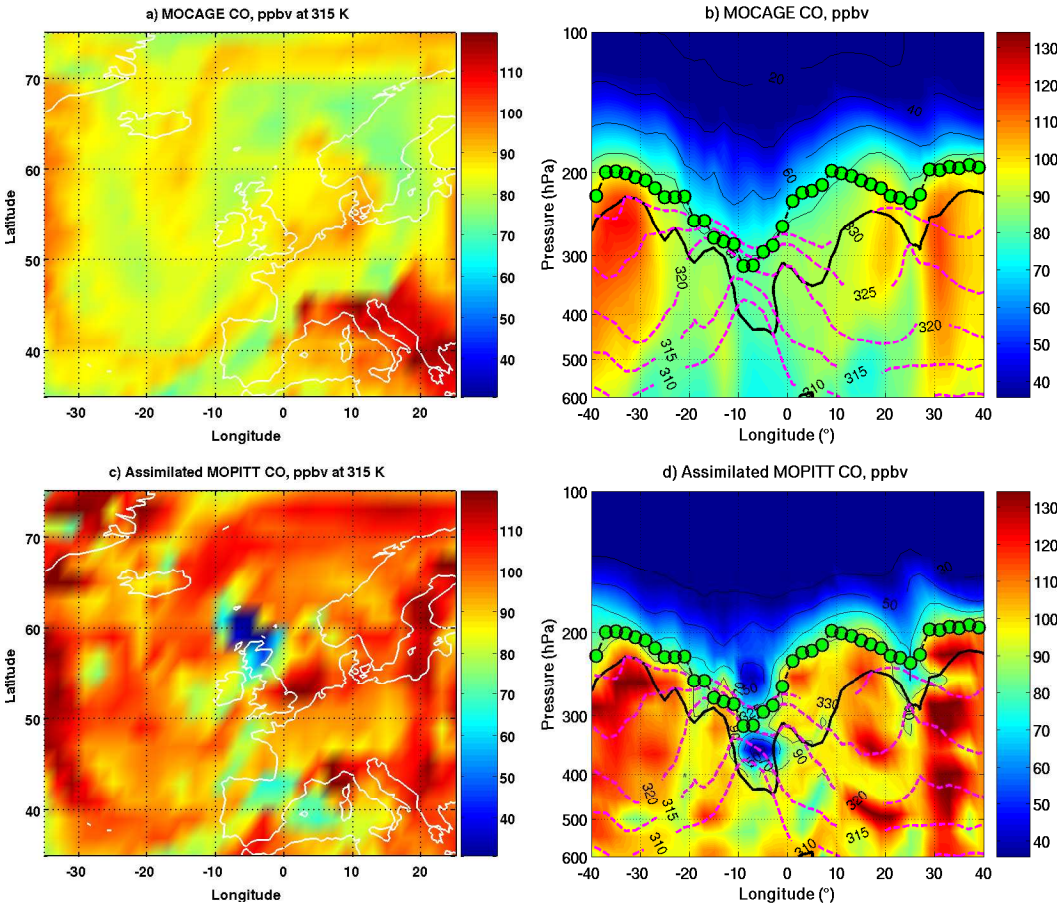


Fig. 13. Same as Fig. 12 but for MOCAGE CO and for MOPITT CO assimilated field in parts per billion by volume (ppbv). In **(b)** and **(d)**, the thick black line corresponds to 1.5 potential vorticity units contour: an estimate of the dynamical tropopause height. The green circles correspond to an estimation of the thermal tropopause height in pressure (hPa) as deduced from lapse rates of ARPEGE temperature profiles. The thermal tropopause has almost the same behaviour as the dynamical tropopause, nevertheless it is higher (see the text for more details).

field at ∼400 hPa (Fig. 7). A large improvement is made by the O_3 assimilated field for which values are 50% to 100% greater than modelled O_3 ones in regions of interest (Fig. 12c). The O_3 assimilated field displays in the 300–200 hPa layer, a maximum with ozone values in excess of 500 ppbv (Fig. 12d), which better fits with the positive ozone anomaly observation (see Fig. 7). On the 315 K isentropic surface where the stratospheric intrusion dives below 400 hPa between 10° W and 0° W, O_3 assimilated field is marginally increased (Fig. 12c, d). This improvement is insufficient to quantitatively reproduce the stratospheric intrusion event. This can be explained by the fact that O_3 retrievals from the MLS sensor are only available above the 215 hPa pressure level and that the information acquired by assimilation has not propagated through atmospheric transport further below the 400 hPa layer in such a very deep stratospheric intrusion. In the next section, we will further describe the STE event representation with the assimilation of CO from MOPITT.

5.2 Signature of the stratospheric intrusion in CO assimilated fields

The 315 K CO distribution from the free run of MOCAGE (Fig. 13a) does not show the expected minima of CO tracing stratospheric intrusions. In the vertical cross-section (Fig. 13b), the lowermost stratosphere between 10° W and 0° W is associated with free run modelled CO values of about 80 ppbv, which are too big to suggest a stratospheric origin. MOPITT CO observations, which are generally sparse and have a low vertical resolution (∼3–4 km) in the UTLS region, lack in principle the spatial and temporal resolutions required to capture stratospheric intrusion events, for which the synoptic variability is quite important. However, the assimilation of MOPITT observations and the transport greatly improve the distribution of CO in the UTLS region as demonstrated by the ability of the run with assimilation to capture signatures of stratospheric intrusions. The CO assimilated field distribution at 315 K (Fig. 13c) obviously exhibits

an intense minimum of CO (<60 ppbv) north of UK where the ozonesonde measurements (see Fig. 1) indicate a very low tropopause overhanging a tropopause fold, in agreement with the potential vorticity maximum on the 315 K surface (Fig. 2 top). In the vertical cross section (Fig. 13d), the distribution of the assimilated CO field has been improved in the tropopause region, which is bounded by the dynamical tropopause (1.5 pvu isoline) and the thermal tropopause deduced from lapse rates of ARPEGE temperature profiles. A minimum of assimilated CO nicely fits within the stratospheric intrusion down to 400 hPa between 10° W and 0° W. At longitudes of upper level ridges with a higher tropopause (35° W, 10° E, and 35° E), the CO assimilated field displays high values compared to the free model run field (Fig. 13b, d) up to the thermal tropopause. The thermal tropopause has almost the same behaviour as the dynamical tropopause, nevertheless it is higher. This is in accordance with the finding of Kim et al. (2001). The thermal tropopause is strongly influenced by uplift vertical motion, whereas the dynamical tropopause is more influenced by downward motion. This explains the large CO concentration observed above the dynamical tropopause. This could be the consequence of the uplift vertical air motion which modify the height of the thermal tropopause, whereas the dynamical tropopause changes through diabatic heating such as radiative heating as reported by Kim et al. (2001). Indeed, the stratospheric intrusion event located between 10° W and 0° W is better represented by the dynamical tropopause. Discussions about the difference between the thermal and the dynamical tropopauses are beyond the scope of this paper. For more explanations, the reader is referred to e.g. Kim et al. (2001); Wirth (2001) and references therein. A possible perspective of this study is a further investigation of processes contributing to the observation of a mixing layer at the tropopause.

Finally, a relative minimum of CO assimilated field stretching out from over western Spain to Brittany (northwest of France) (Fig. 13c) also fits well with the potential vorticity strip (Fig. 2 top). This has been described in Sect. 3 as the dynamical signature of a tropopause fold developing beneath the jet streak over western Europe (Fig. 3c). Signatures of this tropopause fold in the run with assimilation are further described. As suggested by the 1.5 pvu contour in a vertical cross-section at 45° N (Fig. 14b), the tropopause fold develops down to 500 hPa. The CO assimilated field, which is consistent with the upper-level dynamics, with values less than 70 ppbv, has been transported down to below 300 hPa, whereas the CO values from the free model run exceed 80 ppbv at the same location (not shown). The O_3 assimilated field (Fig. 14a) shows ozone values greater than 200 ppbv inside the tropopause fold down to 350 hPa, whereas modelled free run of O_3 values larger than 200 ppbv stay above 150 hPa in the run without assimilation (not shown).

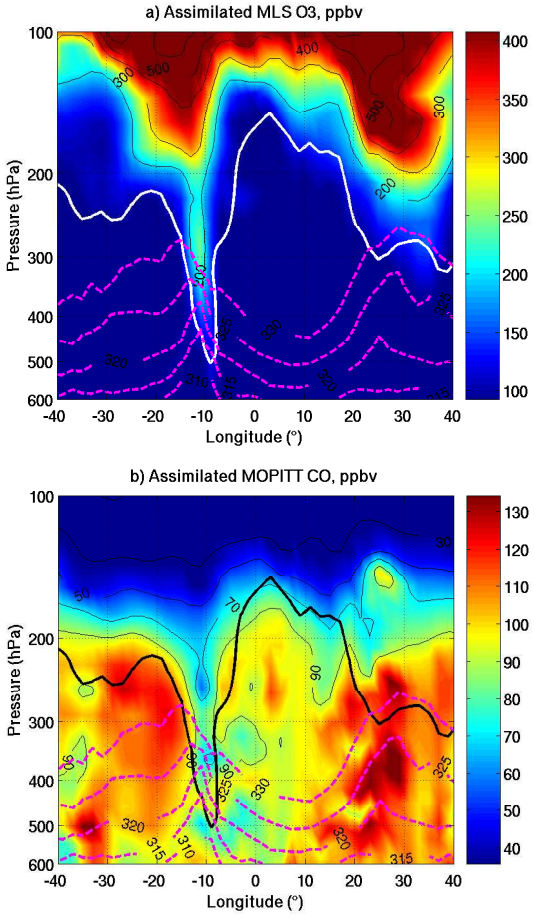


Fig. 14. Zonal cross-section in longitude versus pressure at 45° N between 40° W and 40° E in longitude, and between 600 and 100 hPa in the vertical for **(a)** MLS O_3 assimilated field and **(b)** MOPITT CO assimilated field. The thick lines (white in **(a)** and black in **(b)**) correspond to 1.5 potential vorticity units contour which is an estimate of the dynamical tropopause height. Units of O_3 and CO: parts per billion by volume (ppbv).

6 Conclusions

In this study, by using the global chemical transport model of Météo-France MOCAGE, we demonstrate the capability of assimilated fields of MLS O_3 and MOPITT CO observations to better describe the upper troposphere and lower stratosphere (UTLS) region and a stratosphere-troposphere exchange (STE) event in comparison with modelled free run of O_3 and CO fields. The novel result of this study demonstrates the usefulness of assimilated fields of CO retrieved from a tropospheric measurement sensor, such as MOPITT, in a STE event.

The assimilated products for both O_3 and CO revealed an improvement compared to the free model run results. They have been validated using independent MOZAIC aircraft measurements in terms of vertical profiles as well as total columns in comparison with OMI and AIRS instruments for O_3 and CO, respectively.

In the UTLS region, the O_3 bias, RMS and correlation coefficient between aircraft and assimilated field are −11.5 ppbv, 22.4 ppbv and 0.93, respectively, whereas between aircraft and the free model run they are 33 ppbv, 38.5 ppbv and 0.83, respectively. For CO, the bias, RMS and correlation coefficient between aircraft and assimilated field are −3.16 ppbv, 13 ppbv and 0.79, respectively, whereas between aircraft and the free model run they are 6.3 ppbv, 16.6 ppbv and 0.71, respectively.

In terms of CO vertical profile, the comparison was conducted over the only two MOZAIC airports visited over the whole assimilation period, Frankfurt-Germany and London-UK. Over Frankfurt, the bias, RMS and correlation coefficient between MOZAIC and assimilated CO are 3.3 ppbv, 7.6 ppbv and 0.95, respectively whereas between MOZAIC and modelled CO they are 10.4 ppbv, 8.1 ppbv and 0.89, respectively. Over London, the bias, RMS and correlation coefficient between MOZAIC and assimilated CO are 4.5 ppbv, 8.5 ppbv and 0.63, respectively whereas between MOZAIC and modelled CO they are 12.4 ppbv, 11.7 ppbv and 0.55, respectively.

In terms of total columns, the comparison between CO assimilated field and AIRS data revealed very good qualitative agreement. Indeed, the correlation coefficient is 0.75 and 0.51 between AIRS and assimilated field and between AIRS and modelled field, respectively. For O_3, the average bias between total columns from OMI and assimilated field is negative with a value of −13.21 DobsonUnit (DU) and a corresponding RMS of 12.10 DU, and a correlation coefficient of 0.82, whereas the average bias between total columns from OMI and modelled field is positive with a value of 17.64 DU and a corresponding RMS of 12.82 DU, and a correlation coefficient of 0.66.

These validation exercises have revealed a generally good agreement between assimilated fields and different independent data either in terms of vertical profiles or total columns.

The studied stratospheric intrusion event occurred on 15 August 2007 over the British Isles and was accompanied by an intense tropopause folding. It was documented using meteorological analyses from the ARPEGE model, the global operational weather prediction model of Météo-France. The signature of this event has been verified using the vertical distribution of ozonesonde measurements over Lerwick, UK. Both MLS O_3 and MOPITT CO measurements lack the spatial and the temporal resolutions required to characterize the synoptic variations of the event. Moreover, O_3 MLS observations are only valid from 215 hPa up to the upper stratosphere, which is a strong limitation to reproduce deep stratospheric intrusions into the troposphere. Owing to its good dynamical forcing, the free model run provides rather realistic O_3 and CO vertical distributions. However, modelled O_3 and CO do not reproduce the features of the deep intrusion observed in this study. Assimilated data from MLS improve the representation of O_3 in the UTLS region, nevertheless this improvement is not sufficient enough to reproduce the intensity and the depth of the stratospheric intrusion event well. In contrast, assimilated CO data from MOPITT succeed in capturing the deep structure of the event both horizontally and vertically. The behaviour of CO assimilated fields is consistent with the synoptic evolution of the meteorological parameters in the UTLS region. This is in accordance with the fact that CO is a good tracer in this region, where complex dynamical and chemical processes occur.

Finally, it should be noted that the results of this work open new perspectives for using assimilated MOPITT CO data in STE studies. At this step, we are able to combine measurements from different sensors including their own uncertainties and vertical resolutions. As a particular perspective, we will focus on the quantification of the contribution of each assimilated species (O_3 and CO) in the mixing process between the troposphere and the stratosphere in the UTLS. Data assimilation of chemical observations from different sensors will then be needed for a quantitative representation of chemical species as well as their mixing in the UTLS region.

Acknowledgements. This work is funded in France by the Centre National de Recherches Météorologiques (CNRM) of Météo-France and the Centre National de Recherches Scientifiques (CNRS). We also thank the ECMWF for providing the ozonesonde data. The authors acknowledge for the strong support of the European Commission, Airbus, and the Airlines (Lufthansa, Austrian, Air France) who carry free of charge the MOZAIC equipment and perform the maintenance since 1994. MOZAIC is presently funded by INSU-CNRS (France), Météo-France, and Forschungszentrum (FZJ, Julich, Germany). The MOZAIC data based is supported by ETHER (CNES and INSU-CNRS). ETHER and the Région Midi-Pyrénées are also acknowledged.

Edited by: W. Lahoz



The publication of this article is financed by CNRS-INSU.

References

Appenzeller, C., Davies, H. C., and Norton, W. A.: Fragmentation of stratospheric intrusions, J. Geophys. Res., 101(D1), 1435–1456, 1996.

Aumann, H. H., Chahine, M. T., Gautier, C., Goldberg, M., Kalnay, E., McMillin, L., Revercomb, H., Rosenkranz, P. W., Smith, W. L., Staelin, D., Strow, L., and Susskind, J.: AIRS/AMSU/HSB on the Aqua Mission: Design, Science Objectives Data Products and Processing Systems, IEEE T. Geosci. Remote, 41, 253–264, 2003.

Bencherif, H., El Amraoui, L., Semane, N., Massart, S., Vidyaranya Charyulu, D., Hauchecorne, A., and Peuch, V.-H: Examination of the 2002 major warming in the southern hemisphere using ground-based and Odin/SMR assimilated data: stratospheric ozone distributions and tropic/mid-latitude exchange, Can. J. Phys., 85, 1287–1300, doi:10.1139/P07-143, 2007.

Bennett, A. F.: Inverse Methods in Physical Oceanography, Cambridge University Press., Canada, 346 pp., 1992.

Bousserez, N., Attié, J. L., Peuch, V. H., Michou, M., Pfister, G., Edwards, D., Emmons, L., Mari, C., Barret, B., Arnold, S. R., Heckel, A., Richter, A., Schlager, H., Lewis, A., Avery, M., Sachse, G., Browell, E. V., and Hair, J. W.: Evaluation of the MOCAGE chemistry transport model during the ICARTT/ITOP experiment, J. Geophys. Res., 112, D10S42, doi:10.1029/2006JD007595, 2007.

Brioude, J., Cammas, J.-P., and Cooper, O. R.: Stratosphere-troposphere exchange in a summertime extratropical low: analysis, Atmos. Chem. Phys., 6, 2337–2353, 2006, http://www.atmos-chem-phys.net/6/2337/2006/.

Brioude, J., Cammas, J.-P., Cooper, O. R., and Nedelec, P.: Characterization of the composition, structure, and seasonal variation of the mixing layer above the extratropical tropopause as revealed by MOZAIC measurements, J. Geophys. Res., 113, D00B01, doi:10.1029/2007JD009184, 2008.

Browell, E. V., Gregory, G. L., Beck, S. M., Danielsen, E. F., and Ismail, S.: Tropopause fold structure determined from airborne lidar and in situ measurements, J. Geophys. Res., 92, 2112–2120, 1987.

Cammas, J.-P. and Volz-Thomas, A.: The MOZAIC program (1994–2007), International Global Atmospheric Chemistry (IGAC) Newsletter, Issue N. 37, online available at: http://www.igac.noaa.gov/newsletter/index.php, November, 2007.

Cathala, M.-L., Pailleux, J., and Peuch, V. -H.: Improving chemical simulations of the upper troposphere – lower stratosphere with sequential assimilation of MOZAIC data, Tellus, 55B, 1–10, 2003.

Clark, H. L., Cathala, M.-L., Teyssèdre, H., Cammas, J.-P., and Peuch, V.-H.: Cross-tropopause fluxes of ozone unsing assimilation of MOZAIC observations in a global CTM, Tellus, 59B, 39–49, 2007.

Courtier, P., Freydier, C., Geleyn, J.-F., Rabier, F., and Rochas, M.: The ARPEGE project at Météo–France, in: Workshop on numerical methods in atmospheric models, Vol. 2, 193–231, 1991.

Danielsen, E. F.: Stratospheric-tropospheric exchange based on radioactivity, ozone and potential vorticity, J. Atmos. Sci., 25, 502–508, 1968.

Davies, T. D. and Schuepbach, E.: Episodes of high ozone concentrations at the earth's surface resulting from transport down from the upper troposphere/lower stratosphere: A review and case studies, Atmos. Environ., 28(1), 53–68, 1994.

Deeter, M. N., Emmons, L. K., Francis, G. L., Edwards, D. P., Gille, J. C., Warner, J. X., Khattatov, B., Ziskin, D., Lamarque, J.-F., Ho, S.-P., Yudin, V., Attié, J.-L., Packman, D., Chen, J., Mao, D., and Drumond, J. R.: Operational carbon monoxide retrieval algorithm and selected results for the MOPITT instrument, J. Geophys. Res., 108(D14), 4399, doi:10.1029/2002JD003186, 2003.

Dessler, A. E., Hintsa, E. J., Weinstock, E. M., Anderson, J. G., and Chan, K. R.: Mechanisms controlling water vapor in the lower stratosphere: "A tale of two stratospheres", J. Geophys. Res., 100(D11), 23167–23176, 1995.

Drummond, J. R. and Mand, G. S.: The measurements of pollution in the troposphere (MOPITT) instrument: Overall performance and calibration requirements, J. Atmos. Ocean. Tech., 13, 314–320, 1996.

Dufour, A., Amodei, M., Ancellet, G., and Peuch, V.-H.: Observed and modelled "chemical weather" during ESCOMPTE, Atmos. Res., 74, 161–189, 2004.

Eisele, H., Scheel, H. E., Sladkovic, R., and Trickl, T.: High-resolution lidar measurements of stratosphere-troposphere exchange, J. Atmos. Sci., 56, 319–330, 1999.

El Amraoui, L., Ricaud, P., Urban, J., Théodore, B., Hauchecorne, A., Lautié, N., De La Noe, J., Guirlet, M., Le Flochmoen, E., Murtagh, D., Dupuy, E., Frisk, U., and d'Andon, O. F.: Assimilation of Odin/SMR O_3 and N_2O measurements in a three-dimensional chemistry transport model, J. Geophys. Res., 109, D22304, doi:10.1029/2004JD004796, 2004.

El Amraoui, L., Peuch, V.-H., Ricaud, P., Massart, S., Semane, N., Teyssèdre, H., Cariolle, D., and Karcher, F.: Ozone loss in the 2002/03 Arctic vortex deduced from the Assimilation of Odin/SMR O_3 and N_2O measurements: N_2O as a dynamical tracer, Q. J. Roy. Meteor. Soc., 134, 217–228, 2008a.

El Amraoui, L., Semane, N., Peuch, V.-H., and Santee, M. L.: Investigation of dynamical processes in the polar stratospheric vortex during the unusually cold winter 2004/2005, Geophys. Res. Lett., 35, L03803, doi:10.1029/2007GL031251, 2008b.

Emmons, L. K., Deeter, M. N., Edwards, D. P., Gille, J. C., Attié, J.-L., Warner, J., Ziskin, D., Francis, G., Khattatov, B., Yudin, V., Lamarque, J.-F., Ho, S.-P., Mao, D., Chen, J. S., Drummond, J., Novelli, P., Sachse, G., Coffey, M. T., Hannigan, J. W., Gerbig, C., Kawakami, S., Kondo, Y., Takegawa, N., Schlager, H., Baehr, J., and Ziereis, H.: Validation of MOPITT CO retrievals with aircraft in situ profiles, J. Geophys. Res., 109(D3), D03309, doi:10.1029/2003JD004101, 2004.

Emmons, L. K., Edwards, D. P., Deeter, M. N., Gille, J. C., Campos, T., Ndlec, P., Novelli, P., and Sachse, G.: Measurements of Pollution In The Troposphere (MOPITT) validation through 2006, Atmos. Chem. Phys., 9, 1795–1803, 2009, http://www.atmos-chem-phys.net/9/1795/2009/.

Fisher, M. and Andersson, E.: Developments in 4D-Var and Kalman Filtering, in: Technical Memorandum Research Department, 347, ECMWF, Reading, UK, 2001.

Geer, A. J., Lahoz, W. A., Bekki, S., Bormann, N., Errera, Q., Eskes, H. J., Fonteyn, D., Jackson, D. R., Juckes, M. N., Massart, S., Peuch, V.-H., Rharmili, S., and Segers, A.: The ASSET intercomparison of ozone analyses: method and first results, Atmos. Chem. Phys., 6, 5445–5474, 2006, http://www.atmos-chem-phys.net/6/5445/2006/.

Gouget, H., Vaughan, G., Marenco, A., and Smit, H. G. J.: Decay of a cut-off low and contribution to stratosphere-troposphere exchange, Q. J. Roy. Meteor. Soc., 126, 1117–1141, 2000.

Hintsa, E. J.: Troposphere-to-stratosphere transport in the lowermost stratosphere from measurements of H_2O, CO_2, N_2O and O_3, Geophys. Res. Lett., 25(14), 2655–2658, 1998.

Holton, J. R., Haynes, P. H., McIntyre, M. E., Douglass, A. R., Rood, R. B., and Pfister, L.: Stratosphere-troposphere exchange, Rev. Geophys., 33, 403–439, 1995.

Hoor, P., Fischer, H., Lange, L., Lelieveld, J., and Brunner, D.: Seasonal variations of a mixing layer in the lowermost stratosphere as identified by the CO-O_3 correlation from in situ measurements, J. Geophys. Res., 107(D5), 4044, doi:10.1029/2000JD000289, 2002.

Hoskins, B. J., McIntyre, M. E., and Robertson, A. W.: On the use and significance of isentropic potential vorticity maps, Q. J. Roy. Meteor. Soc., 111, 877–946, 1985.

Hsu, J., Prather, M. J., and Wild, O.: Diagnosing the stratosphere-to-troposphere flux of ozone in a chemistry transport model, J. Geophys. Res., 110, D19305, doi:10.1029/2005JD006045, 2005.

Josse, B., Simon, P., and Peuch, V.-H.: Radon global simulation with the multiscale chemistry trasnport model MOCAGE, Tellus, 56, 339–356, 2004.

Kentarchos, A. S., Roelofs, G. J., and Lelieveld, J.: Model study of a stratospheric intrusion event at lower midlatitudes associated with the development of a cutoff low, J. Geophys. Res., 104(D1), 1717–1728, 1999.

Keyser, D. and Shapiro, M. A.: A review of the structure and dynamics of upper-level frontal zones, Mon. Weather Rev., 114, 452–499, 1986.

Khattatov, B. V., Lamarque, J.-F., Lyjak, L., Menard, R., Levelt, P., Tie, X., Brasseur, G., and Gille, J.: Assimilation of satellite observations of long-lived chemical species in global chemistry transport models, J. Geophys. Res., 105, 29135–29144, 2000.

Kim, K.-E., Jung, E.-S., Campistron, B., and Heo, B.-H.: A physical examination of tropopause height and stratospheric air intrusion – A case study, J. Meteorol. Soc. Jpn., 79, 1093–1103, 2001.

Lagarde, T., Piacentini, A., and Thual, O.: A new representation of data-assimilation methods: The PALM flow-charting approach, Q. J. Roy. Meteor. Soc., 127(571), 189–207, 2001.

Lahoz, W. A., Geer, A. J., Bekki, S., Bormann, N., Ceccherini, S., Elbern, H., Errera, Q., Eskes, H. J., Fonteyn, D., Jackson, D. R., Khattatov, B., Marchand, M., Massart, S., Peuch, V.-H., Rharmili, S., Ridolfi, M., Segers, A., Talagrand, O., Thornton, H. E., Vik, A. F., and von Clarmann, T.: The Assimilation of Envisat data (ASSET) project, Atmos. Chem. Phys., 7, 1773–1796, 2007a, http://www.atmos-chem-phys.net/7/1773/2007/.

Lahoz, W. A., Errera, Q., Swinbank, R., and Fonteyn, D.: Data assimilation of stratospheric constituents: a review, Atmos. Chem. Phys., 7, 5745–5773, 2007b, http://www.atmos-chem-phys.net/7/5745/2007/.

Law, K. S., Plantevin, P.-H., Thouret, V., Marenco, A., Asman, W., Lawrence, M., Crutzen, P., Muller, J.-F., Hauglustaine, D., and Kanakidou, M.: Comparison between global chemistry transport model results and measurements of ozone and water vapor by airbus in-service aircraft (MOZAIC) data, J. Geophys. Res., 105, 1503–1526, 2000.

Lefèvre, F., Brasseur, G. P., Folkins, I., Smith, A. K., and Simon, P.: Chemistry of the 1991–92 stratospheric winter: three dimensional model simulations, J. Geophys. Res., 99, 8183–8195, 1994.

Levelt, P. F., Hilsenrath, E., Leppelmeier, G. W., van den Oord, G. H. J., Bhartia, P. K., Taminnen, J., de Haan, J. F., and Veefkind, J. P.: Science objectives of the ozone monitoring instrument, IEEE T. Geosci. Remote, 44(5), 1283–1287, 2006.

Marenco, A., Thouret, V., Nédélec, P., Smit, H., Helten, M., Kley, D., Karcher, F., Simon, P., Law, K., Pyle, J., Poschmann, G., Von Wrede, R., Hume, C., and Cook, T.: Measurement of ozone and water vapor by Airbus in-service aircraft: The MOZAIC airborne program, An overview, J. Geophys. Res., 103(D19), 25631–25642, 1998.

Massart, S., Piacentini, A., Cariolle, D., El Amraoui, L., and Semane, N.: Assessment of the quality of the ozone measurements from the Odin/SMR instrument using data assimilation, Can. J. Phys., 85, 1209–1223, doi:10.1139/P07-124, 2007.

McMillan, W. W., Barnet, C., Strow, L., Chahine, M., Warner, J., McCourt, M., Novelli, P., Korontzi, S., Maddy, E., and Datta, S.: Daily global maps of carbon monoxide from NASA's atmospheric infrared sounder, Geophys. Res. Lett., 32, L11801, doi:10.1029/2004GL021821, 2005.

Michou, M., Laville, P., Serca, D., Fotiadi, A., Bouchou, P., and Peuch, V.-H.: Measured and modeled dry deposition velocities over the ESCOMPTE area, Atmos. Res., 74, 89–116, doi:10.1016/j.atmosres.2004.04.011, 2005.

Nedelec, P., Cammas, J.-P., Thouret, V., Athier, G., Cousin, J.-M., Legrand, C., Abonnel, C., Lecoeur, F., Cayez, G., and Marizy, C.: An improved infrared carbon monoxide analyser for routine measurements aboard commercial Airbus aircraft: technical validation and first scientific results of the MOZAIC III programme, Atmos. Chem. Phys., 3, 1551–1564, 2003, http://www.atmos-chem-phys.net/3/1551/2003/.

Pan, L. L., Bowman, K. P., Shapiro, M., Randel, W. J., Gao, R. S., Campos, T., Davis, C., Schauffler, S., Ridley, B. A., Wei, J. C., and Barnet, C.: Chemical behavior of the tropopause observed during the Stratosphere-Troposphere Analyses of Regional Transport experiment J. Geophys. Res., 112, D18110, doi:10.1029/2007JD008645, 2007.

Papayannis, A., Balis, D., Zanis, P., Galani, E., Wernli, H., Zerefos, C., Stohl, A., Eckhardt, S., and Amiridis, V.: Sampling of an STT event over the Eastern Mediterranean region by lidar and electrochemical sonde, Ann. Geophys., 23, 2039–2050, 2005, http://www.ann-geophys.net/23/2039/2005/.

Peuch, V.-H., Amodei, M., Barthet, T., Cathala, M. L., Josse, B., Michou, M., and Simon, P.: MOCAGE, MOdèle de Chimie Atmosphérique à Grande Echelle, in: Proceedings of Météo-France: Workshop on atmospheric modelling, 33–36, December 1999.

Pradier, S., Attié, J.-L., Chong, M., Escobar, J., Peuch, V.-H., Lamaraque, J.-F., Kattatov, B., and Edwards, D.: Evaluation of 2001 springtime CO transport over West Africa using MOPITT CO measurements assimilated in a global chemistry transport model, Tellus, 58B, 163–176, 2006.

Rao, T. N. and Kirkwood, S.: Characteristics of tropopause folds over Arctic latitudes, J. Geophys. Res., 110, D18102, doi:10.1029/2004JD005374, 2005.

Ricaud, P., Attié, J.-L., Teyssèdre, H., El Amraoui, L., Peuch, V.-H., Matricardi, M., and Schluessel, P.: Equatorial total column of nitrous oxide as measured by IASI on MetOp-A: implications for transport processes, Atmos. Chem. Phys., 9, 3947–3956, 2009a, http://www.atmos-chem-phys.net/9/3947/2009/.

Ricaud, P., Pommereau, J.-P., Attié, J.-L., Le Flochmoën, E., El Amraoui, L., Teyssèdre, H., Peuch, V.-H., Feng, W., and Chipperfield, M. P.: Equatorial transport as diagnosed from nitrous oxide variability, Atmos. Chem. Phys., 9, 8173–8188, 2009b, http://www.atmos-chem-phys.net/9/8173/2009/.

Santer, B. D., Wehner, M. F., Wigley, T. M. L., Sausen, R., Meehl, G. A., Taylor, K. E., Ammann, C., Arblaster, J., Washington, W. M., Boyle, J. S., and Bruggemann, W., Contributions of anthropogenic and natural forcing to recent tropopause height changes, Science, 301(5632), 479–483, 2003.

Seidel, D. J. and Randel, W. J.: Variability and trends in the global tropopause estimated from radiosonde data, J. Geophys. Res., 111, D21101, doi:10.1029/2006JD007363, 2006.

Semane, N., Peuch, V.-H., El Amraoui, L., Bencherif, H., Massart, S., Cariolle, D., Attié, J.-L., and Abida, R.: An observed and analysed stratospheric ozone intrusion over the high Canadian Arctic UTLS region during the summer of 2003, Q. J. Roy. Meteor. Soc., 133(S2), 171–178, doi:10.1002/qj.141, 2007.

Semane, N., Peuch, V.-H., Pradier, S., Desroziers, G., El Amraoui, L., Brousseau, P., Massart, S., Chapnik, B., and Peuch, A.: On the extraction of wind information from the assimilation of ozone profiles in Météo-France 4-D-Var operational NWP suite, Atmos. Chem. Phys., 9, 4855–4867, 2009, http://www.atmos-chem-phys.net/9/4855/2009/.

Shapiro, M. A.: Turbulent mixing within tropopause folds as a mechanism for the exchange of chemical constituents between the stratosphere and troposphere, J. Atmos. Sci., 37, 994–1004, 1980.

Shapiro, M. A., Hampel, T., and Krueger, A. J.: The arctic tropopause fold, Mon. Weather Rev., 115, 444–454, 1987.

Sprenger, M., Maspoli, M. C., and Wernli, H.: Tropopause folds and cross-tropopause exchange: A global investigation based upon ECMWF analysis for the time period March 2000 to February 2001, J. Geophys. Res., 108(D12), 8518, doi:10.1029/2002JD002587, 2003.

Stockwell, W. R., Kirchner, F., Kuhn, M., and Seefeld, S.: A new mechanism for regional atmospheric chemistry modelling, J. Geophys. Res., 102(D22), 25847–25879, 1997.

Stohl, A., Bonasoni, P., Cristofanelli, P., Collins, W., Feichter, J., Frank, A., Forster, C., Gerasopoulos, E., Gaggeler, H., James, P., Kentarchos, T., Kromp-Kolb, H., Kruger, B., Land, C., Meloen, J., Papayannis, A., Priller, A., Seibert, P., Sprenger, M., J. Roelofs, G. J., Scheel, H., E., Schnabel, C., Siegmund, P., Tobler, L., Trickl, T., Wernli, H., Wirth, V., Zanis, P., and Zerefos, C.: Stratosphere-troposphere exchange: A review, and what we have learned from STACCATO, J. Geophys. Res., 108(D12), 8516, doi:10.1029/2002JD002490, 2003.

Susskind, J., Barnet, C. D., and Blaisdell J. M.: Retrieval of atmospheric and surface parameters from AIRS/AMSU/HSB data in the presence of clouds, IEEE T. Geosci. Remote, 41, 390–409, 2003.

Talagrand, O.: A posteriori validation of assimilation algorithms, in: Data Assimilation for the Earth System, NATO ASI Series, edited by: Swinbank, R., Shutyaev, V., and Lahoz, W. A., Kluwer Academic Publishers, Dordrecht, The Netherlands, 85–95, 2003.

Thouret, V., Marenco, A., Logan, J. A., Nédélec, P., and Grouhel, C.: Comparisons of ozone measurements from the MOZAIC airborne program and the ozone sounding network at eight locations, J. Geophys. Res., 103, 25695–25720, 1998.

Warner, J. X., Comer, M. M., Barnet, C. D., McMillan, W. W., Wolf, W., Maddy, E., and Sachse, G.: A Comparison of Satellite Tropospheric Carbon Monoxide Measurements from AIRS and MOPITT During INTEX-A, J.Geophys. Res., 112, D12S17, doi:10.1029/2006JD007925, 2007.

Waters, J. W., Froidevaux, L., Harwood, R. S., Jarnot, R. F., Pickett, H. M., Read, W. G., Siegel, P. H., Cofield, R. E., Filipiak, M. J., Flower, D. A., Holden, J. R., Lau, G. K., Livesey, N. J., Manney, G. L., Pumphrey, H. C., Santee, M. L., Wu, D. L., Cuddy, D. T., Lay, R. R., Loo, M. S., Perun, V. S., Schwartz, M. J., Stek, P. C., Thurstans, R. P., Boyles, M. A., Chandra, S., Chavez, M. C., Chen, G-S., Chudasama, B. V., Dodge, R., Fuller, R. A., Girard, M. A., Jiang, J. H., Jiang, Y., Knosp, B. W., LaBelle, R.C., Lam, J. C., Lee, K. A., Miller, D., Oswald, J. E., Patel, N. C., Pukala, D. M., Quintero, O., Scaff, D. M., Synder, W. V., Tope, M. C., Wagner, P. A., and Walch, M. J.: The Earth Observing System Microwave Limb Sounder (EOS MLS) on the Aura satellite, IEEE T. Geosci. Remote, 44(5), 1075–1092, 2006.

Wernli, H. and Bourqui, M.: A Lagrangian "1-year climatology" of (deep) cross-tropopause exchange in the extratropical northern hemisphere., J. Geophys. Res., 107(D2), 4021, doi:10.1029/2001JD000812, 2002.

Wimmers, A. J., Moody, J. L., Browell, E. V., Hair, J. W., Grant, W. B., Butler, C. F., Fenn, M. A., Schmidt, C. C., Li, J., and Ridley, B. A.: Signatures of tropopause folding in satellite imagery, J. Geophys. Res., 108(D4), 8360, doi:10.1029/2001JD001358, 2003.

Wimmers, A. J. and Moody, J. L.: Tropopause folding at satellite-observed spatial gradients: 2. Development of an empirical model, J. Geophys. Res., 109, D19306, doi:10.1029/2003JD004145, 2004.

Wirth, V.: Cyclone–anticyclone asymmetry concerning the height of the thermal and the dynamical tropopause, J. Atmos. Sci., 58, 26–37, 2001.

World Meteorological Organization (WMO): Atmospheric Ozone 1985, 1, Rep. 16, 1986.

Zahn, A., Brenninkmeijer, C. A. M., Maiss, M., Scharffe, D. H., Crutzen, P., J., Hermann, M., Heintzenberg, J., Wiedensohler, A., Gusten, H., Heinrich, G., Fischer, H., Cuijpers, J. W. M., and van Velthoven, P. F. J.: Identification of extratropical two-way troposphere-stratosphere mixing based on CARIBIC measurements of O_3, CO, and ultrafine particles, J. Geophys. Res., 105(D1), 1527–1535, 2000.